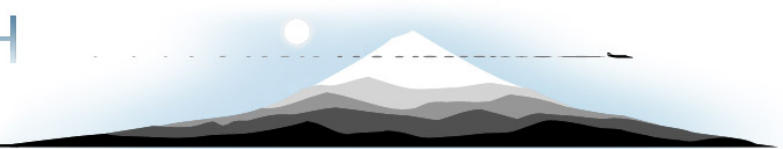


SKY RESEARCH



**Environmental Security Technology Certification Program
(ESTCP)**

Final Report

**Demonstration of Airborne Wide Area Assessment
Technologies at the Toussaint River, Ohio**



**Project No. 200535: Innovative Multi-Sensor Airborne Wide Area
Assessment of UXO Sites**

**April 17, 2007
Version 2.0**

REPORT DOCUMENTATION PAGE*Form Approved
OMB No. 0704-0188*

The public reporting burden for this collection of information is estimated to average 1 hour per response, including the time for reviewing instructions, searching existing data sources, gathering and maintaining the data needed, and completing and reviewing the collection of information. Send comments regarding this burden estimate or any other aspect of this collection of information, including suggestions for reducing the burden, to the Department of Defense, Executive Services and Communications Directorate (0704-0188). Respondents should be aware that notwithstanding any other provision of law, no person shall be subject to any penalty for failing to comply with a collection of information if it does not display a currently valid OMB control number.

PLEASE DO NOT RETURN YOUR FORM TO THE ABOVE ORGANIZATION.

1. REPORT DATE (DD-MM-YYYY)		2. REPORT TYPE		3. DATES COVERED (From - To)	
4. TITLE AND SUBTITLE				5a. CONTRACT NUMBER	
				5b. GRANT NUMBER	
				5c. PROGRAM ELEMENT NUMBER	
6. AUTHOR(S)				5d. PROJECT NUMBER	
				5e. TASK NUMBER	
				5f. WORK UNIT NUMBER	
7. PERFORMING ORGANIZATION NAME(S) AND ADDRESS(ES)				8. PERFORMING ORGANIZATION REPORT NUMBER	
9. SPONSORING/MONITORING AGENCY NAME(S) AND ADDRESS(ES)				10. SPONSOR/MONITOR'S ACRONYM(S)	
				11. SPONSOR/MONITOR'S REPORT NUMBER(S)	
12. DISTRIBUTION/AVAILABILITY STATEMENT					
13. SUPPLEMENTARY NOTES					
14. ABSTRACT					
15. SUBJECT TERMS					
16. SECURITY CLASSIFICATION OF:			17. LIMITATION OF ABSTRACT	18. NUMBER OF PAGES	19a. NAME OF RESPONSIBLE PERSON
a. REPORT	b. ABSTRACT	c. THIS PAGE			19b. TELEPHONE NUMBER (Include area code)

Table of Contents

Table of Contents	ii
List of Figures.....	iii
List of Tables	iii
Acronyms	iv
1. Introduction.....	1
1.1. Background	1
1.2. Objectives of the Demonstration	1
1.3. Regulatory Drivers.....	2
1.4. Stakeholder/End-User Issues	3
2. Technology Description	4
2.1. Technology Development and Application.....	4
2.2. Previous Testing of the Technology.....	9
2.3. Factors Affecting Cost and Performance	9
2.4. Advantages and Limitations of the Technology.....	9
3. Demonstration Design	11
3.1. Performance Objectives	11
3.2. Selecting Test Site	11
3.3. Test Site History/Characteristics.....	11
3.4. Pre-Demonstration Testing and Analysis	16
3.5. Testing and Evaluation Plan	17
4. Performance Assessment.....	23
4.1. Data Calibration Results	23
4.2. Anomaly Picking	26
4.3. Performance Criteria.....	31
4.4. Performance Confirmation Methods	31
5. Cost Assessment	35
5.1. Cost Reporting	35
5.2. Cost Analysis	36
6. Implementation Issues	38
6.1. Regulatory and End-User Issues	38
7. References.....	39
8. Points of Contact.....	40
Appendix A: Comparison on NRL DAS with Bell and Sky Hardware DAS with Hughes 500	A-1
Appendix B: Recovered Target Results.....	B-1

List of Figures

Figure 1.	Former Erie Army Depot and vicinity with HeliMag survey area outlined in red.	2
Figure 2.	Sky Research, Inc. MD 530F helicopter and magnetometer boom assembly	4
Figure 3.	HeliMag sensor boom diagram.....	6
Figure 4.	Sky Research, Inc. DAS.....	7
Figure 5.	Erosion prevention measures along shoreline.....	15
Figure 6.	Terrestrial vegetation.	15
Figure 7.	Helicopter MTADS processing flow chart	20
Figure 8.	Calibration line target positioning errors	24
Figure 9.	Dipole fit size estimates for calibration line targets	25
Figure 10.	Dipole fit solid angle estimate for calibration line targets	25
Figure 11.	Target anomalies selected within the survey area and their densities	27
Figure 12.	Minimum detectable ordnance size as a function of the separation distance between the sensor and the target.	28
Figure 13.	Distribution of dipole fit size estimates	29
Figure 14.	Recovered moments of 155 mm targets identified during the intrusive investigation	30
Figure 15.	Histogram of sensor altitude above the water	33

List of Tables

Table 1.	Sky Research HeliMag Components	5
Table 2.	Performance Objectives	12
Table 3.	Compilation of Munitions Found in Previous Activities.....	13
Table 4.	Standard Deviations of the Bell Helicopter with NRL Data Acquisition Computer and the Hughes Helicopter with the Sky DAS.	16
Table 5.	Emplaced Calibration Targets.....	18
Table 6.	HeliMag Data Collection Acreage	18
Table 7.	Helicopter MTADS Raw Data Input Files.....	21
Table 8.	Calibration Line Results for Calibration Lane targets	23
Table 9.	Performance Criteria for the Toussaint River HeliMag Technology Demonstration	31
Table 10.	Performance Metrics Confirmation Methods and Results.....	34
Table 11.	Cost Tracking.....	36
Table 12.	Points of Contact.....	40

Acronyms

AGL	Above Ground Level
CRADA	Cooperative Research and Development Agreement
cm	centimeter
Cs	Cesium
DAS	Data Acquisition System
DERP	Defense Environmental Restoration Program
DGM	Digital Geophysical Mapping
DoD	Department of Defense
ESTCP	Environmental Security Technology Certification Program
FUDS	Formerly Used Defense Sites
GDC	Geophysical Data Center
GIS	Geographic Information Systems
GPS	Global Positioning System
HeliMag	Helicopter MTADS Magnetometry (see MTADS)
Hz	hertz
IMU	Inertial Measurement Unit
kts	knots
m	meter
m/s	meters per second
μs	microsecond
MEC	Munitions and Explosives of Concern
MRS	Munitions Response Site
MTADS	Multi-Sensor Towed Array Detection System
nT	nanotesla
NRL	Naval Research Lab
RMSE	Root Mean Square Error
RTK GPS	Real-time Kinematic Global Positioning System
TCRA	Time Critical Removal Action
TOA	Time of Applicability
USACE	U.S. Army Corps of Engineers
UTC	Universal Time Coordinated
UTM	Universal Transverse Mercator
UXO	Unexploded Ordnance
WAA	Wide Area Assessment
WAA-PP	Wide Area Assessment-Pilot Program

1. Introduction

1.1. Background

The former Erie Army Depot, Ottawa County, Ohio, is located along the western shore of Lake Erie. This site and the associated impact areas are classified by the United States Government as Formerly Used Defense Sites (FUDS) under the Defense Environmental Restoration Program (DERP). This property was formerly used for artillery testing, resulting in impact areas on land and in Lake Erie. Munitions and explosives of concern (MEC), including potentially live or unexploded ordnance (UXO) have been found on the lake bottom, in the Federal navigation channel at the Toussaint River, in the marshland adjacent to the firing ranges, and along beaches fronting the former Depot. The impact areas were located in, near, or offshore of the FUDS beaches adjacent to Lake Erie. Ordnance found on or near the FUDS shore of Lake Erie appears to be mobile and may have originated from offshore or nearshore impact areas. In FY06, the Environmental Security Technology Certification Program (ESTCP) was directed by Congress to conduct work to characterize UXO contamination impacting the Toussaint River area, and this survey is part of ESTCP's Wide Area Assessment Pilot Program (WAA-PP).

This demonstration utilized Helicopter Multi-Sensor Towed Array Detection System (MTADS) Magnetometry (HeliMag) technology, a wide area assessment (WAA) technology, to assist in the characterization of the shore and shallow areas in and around the Toussaint River relative to munitions contamination from historical activities at the Erie Army Depot and Camp Perry. HeliMag provides efficient low altitude digital geophysical mapping (DGM) capabilities for metal detection and feature discrimination at a resolution approaching that of ground survey methods, limited primarily by terrain, vegetation and structural inhibitions to safe low-altitude flight. This demonstration was conducted under ESTCP MM-0535.

1.2. Objectives of the Demonstration

The purpose of this demonstration was to survey marsh, shallow water and river areas at the site as described by this demonstration plan. Specific objectives of this demonstration included:

- Characterize the marsh, shallow water and river areas in and around the Toussaint River that are contaminated with munitions from historical activities at the Erie Army Depot and Camp Perry, including:
 - Identification of areas of concentrated munitions;
 - Bound the munitions-contaminated areas in Lake Erie and on the adjacent beaches;
 - Estimate density and distribution of munitions types and sizes;
 - Characterize site conditions to support future investigation, prioritization, remediation, and cost estimation tasks.

A determination of success for this demonstration was based on the performance of the system, as described in Section 4.

1.3. Regulatory Drivers

The Toussaint River is situated immediately north of the former Erie Army Depot. This river includes several small craft and commercial fishing marinas. The U.S. Army Corps of Engineers (USACE) - Buffalo District is responsible for maintaining a navigable waterway. The area is periodically dredged, either by the USACE or local private interests. These dredging activities are often affected by munitions encounters. Figure 1 shows the approximate survey area boundaries and mouth of the Toussaint River. This site and the associated impact areas are classified by the United States Government as a FUDS under the DERP.

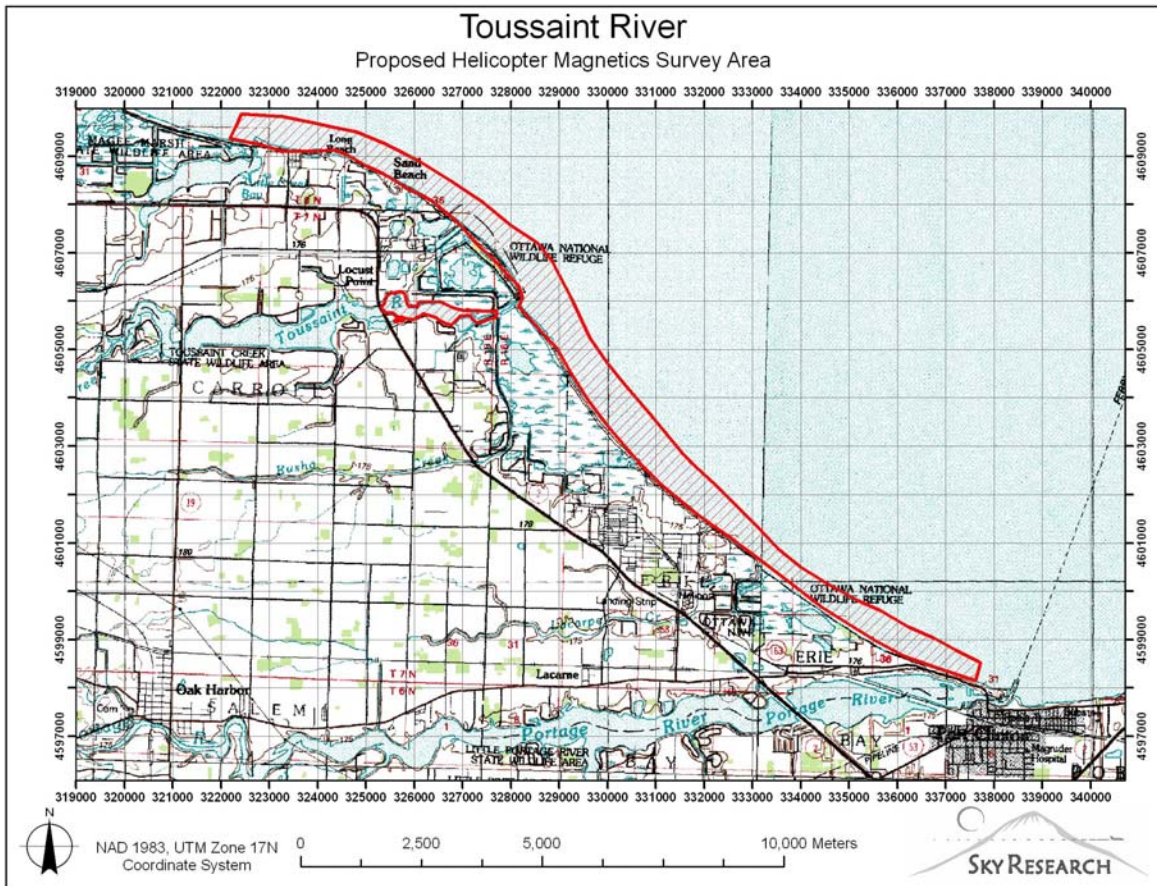


Figure 1. Former Erie Army Depot and vicinity with HeliMag survey area outlined in red.

1.4. Stakeholder/End-User Issues

ESTCP is managing the stakeholder issues as part of its WAA-PP. ESTCP plans to use a process that will ensure that the information generated by the helicopter, water and validation surveys is useful to a broad stakeholder community (e.g., technical project managers and Federal, State, and local governments, as well as other stakeholders).

2. Technology Description

2.1. Technology Development and Application

The Sky Research, Inc. helicopter technology is based on the Naval Research Laboratory (NRL) MTADS technology, transferred to Sky Research for commercialization via a Cooperative Research and Development Agreement (CRADA). Prior to the transfer, this technology was fully evaluated by the Department of Defense (DoD) by ESTCP (Nelson et al., 2005; Tuley and Dieguez, 2005).

The HeliMag system includes a helicopter-borne array of magnetometers and software designed specifically to process data collected with this system and perform physics-based analyses on identified targets. In addition, Sky Research recently completed updates to the NRL MTADS technology to improve performance and reliability of the technology.

2.1.1. Helicopter Platform

Sky Research used a Hughes MD530F helicopter (Figure 2) for data collection at the Toussaint River site, which has greater power and lift than other helicopters of its size. Table 1 presents the airborne MTADS sensor system technologies deployed on the helicopter platform, including:

- Array of seven Geometrics 822 Cesium (Cs) vapor magnetometers
- 2 Trimble MS750 global position system (GPS) receivers
- 1 Optech Laser altimeter
- 4 Acoustic altimeters
- Data acquisition system (DAS)



Figure 2. Sky Research, Inc. MD 530F helicopter and magnetometer boom assembly. Seven magnetometers are contained in the composite-material boom and positioned with the GPS antenna and laser / acoustics altimeters.

Table 1. Sky Research HeliMag Components

Technology Component	Specifications
Geophysical Sensors	7 Geometrics 822 Cs vapor magnetometers, 0.001 nanotesla (nT) resolution
GPS Equipment	2 Trimble MS750 GPS receivers, 2-3 centimeter (cm) horizontal precision
Altimeters	1 Optech laser altimeter and 4 acoustic altimeters, 1 cm resolution
DAS	Sky Research DAS capable of data collection up to 400 hertz (Hz), 10 microsecond (μ Sec) timing precision
Aircraft	Hughes MD 530F helicopter

2.1.2 Sensors and Boom

The MTADS magnetic sensors are seven Geometrics 822A Cs vapor full-field magnetometers (the 822A is a variant of the Geometrics 822 sensor). The array of seven sensors is interfaced to a DAS and the sensors are evenly spaced at 1.5 m intervals on a 9 m Kevlar boom mounted on the helicopter. The new boom design (Figure 3) updates the NRL boom design, with changes including boom placement closer to the helicopter to minimize weight and a quick assembly design that decreases assembly time to two hours. Additional changes in boom design include GPS sensors moved to 7.5 m separation or 3.75 m from centerline to improve fuselage shadowing and new digital acoustic sensors, which eliminate the voltage devices in the NRL system because of their plastic housing, and which have been moved to 4.5 m separation or 2.25 m from centerline.

2.1.3 Positioning Technologies

Sensor positioning is provided using real-time kinematic (RTK) GPS navigation, with real-time position updates at 20 Hz and horizontal accuracy of about 5 cm; the Inertial Measurement Unit (IMU) is used to correct for platform pitch and roll. At typical 1-3 m above ground level (AGL) operating heights, the 5 cm RTK GPS accuracy has been shown on previous deployments to translate to a horizontal positioning error of about < 5 cm root mean square error (RMSE).

The GPS satellite clock time is used to time-stamp both position and sensor data information for merging channel and position data. An onboard navigation guidance display provides pilot guidance, with survey parameters established in a navigation computer that shares the RTK GPS

positioning data stream with the DAS. Pilot steering information (horizontal and vertical) is provided in graphic format. The GPS and altimeter data integrity is presented as a binary status button and the GPS fix quality is indicated via text box as well as by changing the color of the graphic position trace. This allows the operator to respond to both visual cues on the ground and to the survey guidance display. Following a survey, the operator can survey any missed areas before leaving the site.

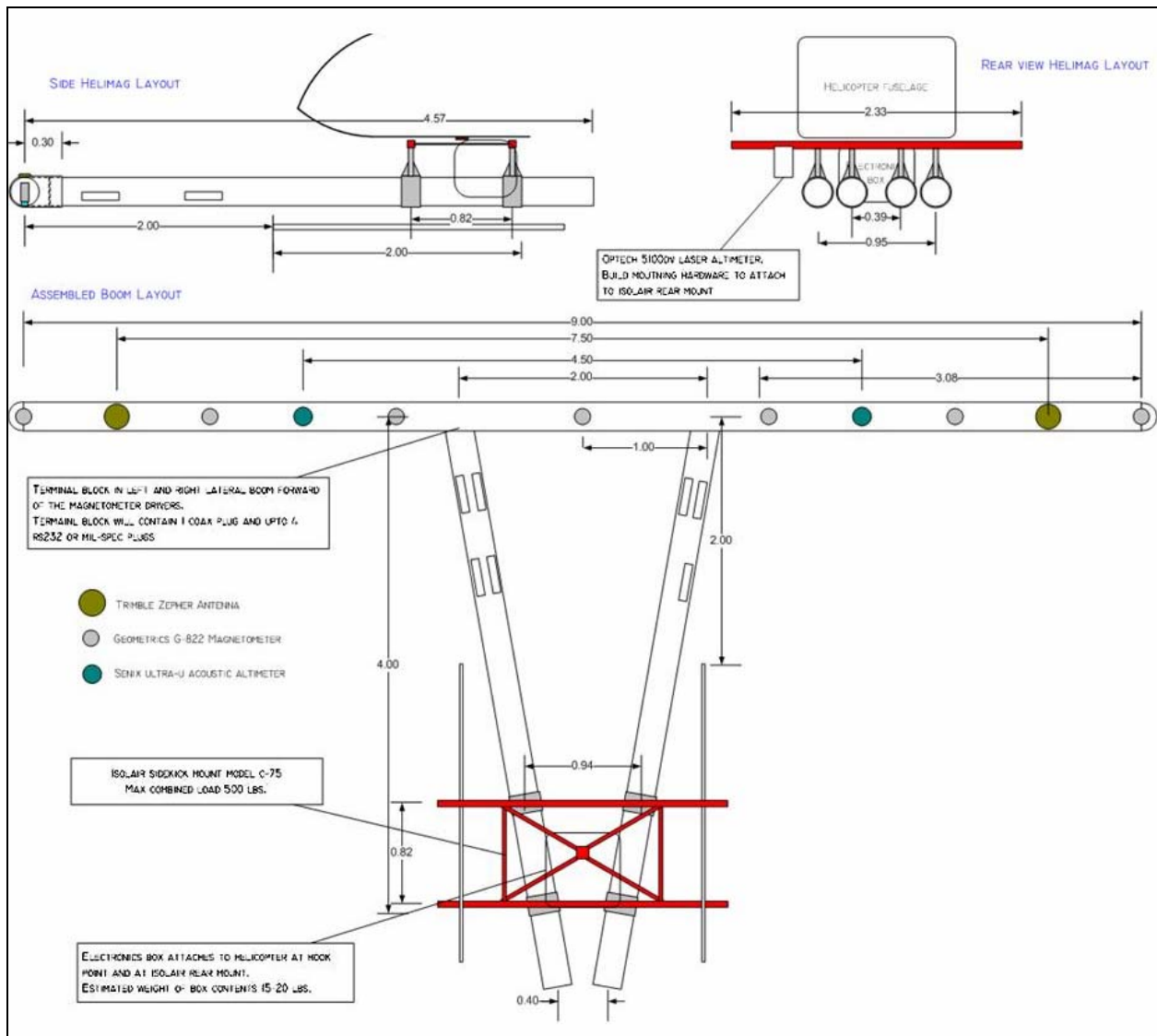


Figure 3. HeliMag sensor boom diagram (2nd GPS antenna not shown).

2.1.4 Data Acquisition System

A new DAS was developed by Sky Research for use with the helicopter system in early 2006 (Figure 4), providing the following advantages over the previous DAS used for WAA-PP projects: smaller footprint (3.5" x 5" x 6"), Linux operating system (Realtime Linux 2.6), more accurate time stamping (10 μ S) and faster sampling rate (400 Hz vs. 100 Hz). The magnetometer data, logged at 400 Hz were down-sampled to 100 Hz, providing a nominal down-the-track sample interval of 0.15 – 0.20 m per sample at a survey speed of 15 – 20 meters per second (m/s) (30 – 40 knots [kts]).

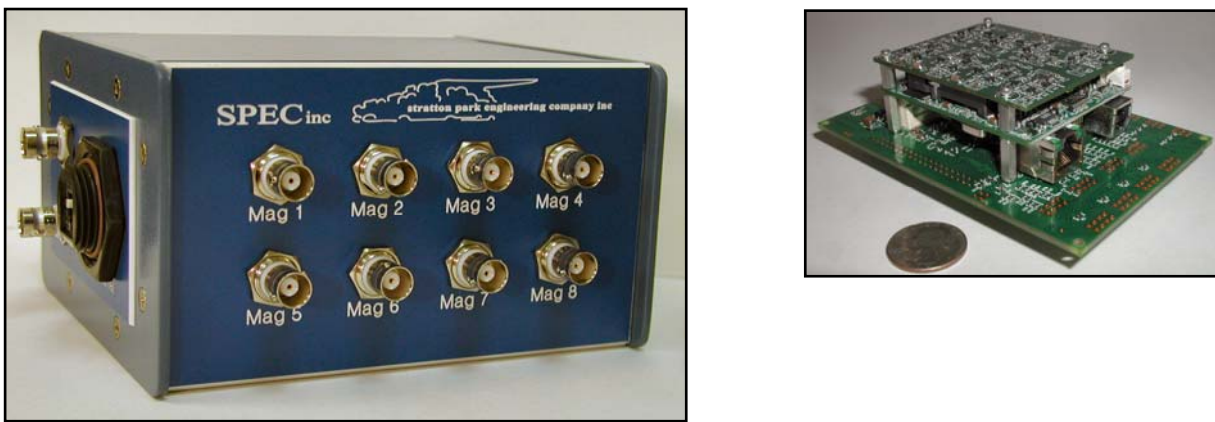


Figure 4. Sky Research, Inc. DAS.

2.1.5 Data Processing

UXOLab software was used for all HeliMag data processing; this software contains all the functionality required to process raw geophysical data, detect anomalous regions and perform geophysical inversions. During the first data processing stage, the raw data for a given survey flight are time-aligned and transcribed from the various raw data files into a 'flight' database. Routines are run to automatically reject or 'default' invalid data. Data are rejected based upon status flags present in the raw data records or, in the case of the magnetometer data, a simple 'in range' test may be used. The GPS geographic position coordinates are transformed to WGS84 Universal Transverse Mercator (UTM) coordinates. At this point the data are visually inspected to ensure both integrity and quality. This pre-processing stage is instrumentation-specific and the steps required to transcribe these data into a time-aligned database are dictated by the structure of the data outputs from each device and the manner in which they are logged. All data outputs are received by the on-board DAS. A DAS time stamp is appended to each sample data string and the sample are then stored in a separate data file for each device.

Data processing with the use of UXOLab greatly speeds up the merging and data interpolating process due to the large database functionality and optimized merging algorithms. Typical production processing for 300-500 acres takes approximately eight hours of data processing to produce a raw data plot image. This image is used to check survey coverage and operation of the system, and is not typically used for target picking. Additional processing steps after this raw data step include filtering, geologic trend removal, and smoothing if needed. Filters are used in the processing of magnetic data to mitigate complicating effects in the data and increase capability to detect discrete buried targets and geologic trend removal is used if geological trends are present. Merged HeliMag sensor and position data files are then converted to magnetic anomaly maps using UXOLab.

2.1.6 Data Analysis

Automatic target selection for large scale surveys such as this one has the advantage of being objective and repeatable as well as much faster than manual selection if a very large number of targets are to be selected. However, automatic target pickers are not yet sophisticated enough to reliably detect closely spaced targets or targets that are at or below the same amplitude as local geologic signal. Furthermore these automated routines are not able to differentiate between our targets of interest and local geologic anomalies, or response from non-UXO like anthropologic sources (e.g. pipelines). In practice, the decision to pick manually, or use an auto-picker then add/reject targets manually, is made based upon the number of targets to be picked and the extent of geologic/anthropologic clutter.

For the purposes of WAA where the main goal is to delineate target density throughout the survey site, the limitations of automatic target selection are not as detrimental as they would be if we were concerned with detecting every possible UXO target. The challenge is to calibrate the automatic target selection routine so that the number of valid targets of interest selected is maximized, while minimizing the number of targets selected due to geologic noise or other noise sources (geologic noise is usually the predominant noise source). To achieve this, a subset of manual target selection results are compared with those obtained using an automated target selection routine over a representative subset of the survey site.

The automatic selection process utilizes the Automated Wavelet Detection Algorithm (Billings and Herrmann, 2003). Individual peaks in the magnetic data are followed across multiple scales, with the decay in peak amplitude related to the depth to the source. Nearby positive and negative peaks in the image are joined together if they have comparable depth estimates. In this way, incorrectly joining the peaks from nearby dipoles that are at different depths can be avoided. In the last stage of the algorithm, the amplitudes of the peaks and their relative position are used to provide an initial estimate of the dipole parameters. The detection thresholds are selected based upon a comparison with manually selected targets as well as the objectives and limitations imposed by the conditions of each specific site.

Filtered sensor data points were interpolated into magnitude surface rasters using geographic information system (GIS)-based interpolation scripts. In addition, inversions were completed on targets selected by the ESTCP Program Office using UXOLab to model the targets as magnetic dipoles controlled by six parameters; target X, Y location, depth, azimuth, inclination, and size. The size is measured as the strength of the dipole source causing the observed magnetic anomaly and is correlated to the specific targets of interest.

2.2. Previous Testing of the Technology

Previous testing of the helicopter magnetometry technology in general was supported by ESTCP (Nelson et al., 2005). The primary development objective was to provide a UXO site characterization capability for extended areas, while retaining substantial detection sensitivity for individual UXO. The system included data collection hardware in the form of a helicopter-borne array of magnetometers and software designed specifically to process data collected with this system and perform physics-based analyses on identified targets.

2.3. Factors Affecting Cost and Performance

For all airborne surveys, the largest single factor affecting the survey costs is the cost of operating the survey aircraft and sensors at the site. These equipment costs are related to capital value, maintenance overhead and direct operating costs of these expensive sensor and aircraft systems. Mobilization to and from the site increases costs as distance increases, and flexibility of scheduling is critical in determining whether mobilization and deployment costs can be shared across projects. In addition, helicopter surveys are limited by topography and vegetation and therefore can be deployed only to sites with suitable conditions.

Another significant cost factor is data volume and the requirement for a robust data processing infrastructure to manage large amounts of digital remote sensing data.

2.4. Advantages and Limitations of the Technology

As with all characterization technologies, site specific advantages and disadvantages exist that dictate the level of success of their application.

Advantages of HeliMag technologies include:

- The ability to characterize very large areas;
- Lower cost as compared to ground based DGM methods.

Limitations of HeliMag technologies include:

- As a WAA tool, not intended to detect individual MEC items;
- Site physiography, such as terrain, soils, and vegetation, can constrain the use of the technology;

- Limited to shallow water areas due to height above target limitations of the technology.

3. Demonstration Design

3.1. Performance Objectives

Performance objectives are a critical component of the demonstration plan because they provide the basis for evaluating the performance and costs of the technology. For the WAA projects, both primary and secondary performance objectives have been established. Table 2 lists the performance objectives for the helicopter MTADS technology, along with criteria and metrics for evaluation, to be documented as a deliverable of this demonstration.

3.2. Selecting Test Site

ESTCP received Congressional direction to study the Toussaint River area. From historic activities at Camp Perry and the former Erie Army Depot, there is a large impact area in the water. In addition, there are other impact areas in the swampy land adjacent to these facilities and Lake Erie. The primary interest of the community is in the UXO that affects dredging of the navigation channel to the river. The helicopter technology was demonstrated on areas of the site that were conducive to low altitude magnetometry in the near shore area, the mouth of the Toussaint River, and the shallow water areas of Lake Erie. These areas encompassed approximately 3,300 acres. An underwater system was demonstrated concurrently at the site and surveyed transects in deeper water areas.

3.3. Test Site History/Characteristics

Camp Perry was established in 1907 by the state of Ohio for the training of the state National Guard. The Erie Army Depot was initially established in 1918 on a portion of the Camp Perry lands as the Camp Perry Proving Grounds, and then designated as the Erie Proving Grounds in support of increased activities during the World War II period. Between 1918 and 1966, this site was used by the U.S. Army for testing and proof-firing artillery and as an ordnance storage and issue center. During that time, in 1951, it was renamed the Erie Army Depot and assumed the additional roles of anti-aircraft support testing and the overhauling of surface-to-air guided missiles during the Korean War. Ordnance tested included small caliber items, artillery, mortar shells up to 240 mm, and rockets.

Activities to remove MEC by the USACE in the early 1990s revealed that ordnance were being transported by lake and river waters to locations outside the impact zones. Dredging activities to maintain the navigable channel of the Toussaint River have exposed MEC (Pope et al., 1996).

A more complete description of the history of the Former Erie Army Depot is presented in the ESTCP Demonstration Plan for the site (ESTCP, 2006) and Pope et al. 1996.

Table 2. Performance Objectives

Type of Performance Objective	Primary Performance Criteria	Expected Performance (Metric)
Primary/Qualitative	Ease of use and efficiency of operations for each sensor system	Efficiency and ease of use meets design specifications
Primary/Quantitative	Geo-reference position accuracy	Horizontal < 0.25 m; Vertical < 0.5 m
Secondary/Quantitative	Survey coverage	>0.95 of planned survey area
Secondary/Quantitative	Operating parameters (altitude, speed, overlap, production level)	Altitude: 1-3 m AGL; Speed: 15 – 20 m/s (30-40 kts); Overlap: 10% Production level: 300 acres/day
Primary/Quantitative	Noise level (combined sensor/platform sources, post-filtering)	<1 nT
Secondary/Quantitative	Data density/point spacing	0.5 m along track 1.5 m cross track
Secondary/Quantitative	Modeling parameter definition (X, Y location; depth; and size)	X,Y Location : 90% within 0.5m; Depth: 90% within 0.5 m; Size: 90% in correct Small/Medium/Large classification

Several previous activities have uncovered a variety of munitions types. These activities have included dredging, a Time Critical Removal Action (TCRA) and a beach removal action. The munitions types are listed in Table 3. In addition to those known to have been fired over the life of the range, it has been anecdotally reported (but unconfirmed) that munitions were dumped from barges in the vicinity of the impact area during the 1960s. The types of munitions and quantities were not documented.

Table 3. Compilation of Munitions Found in Previous Activities

Munition Type	Comments
3.5 inch rocket	Found during dredging
60 mm mortar	Found during dredging and beach removal action and TCRA
106 mm projectile	Found during dredging and beach removal action and TCRA
M52 fuze	Found during dredging
M15 Smoke Grenade	Found during dredging
105 mm projectile	Found during dredging and beach removal action and TCRA
90 mm projectile	Found during dredging and TCRA
20 mm projectile	Found during Beach Removal Action
165 mm	Pieces found during Beach Removal Action
40 mm	Found during TCRA
75 mm	Found during TCRA
81 mm	Found during TCRA
155 mm	Found during TCRA

A number of impact areas in Lake Erie were established in order to conduct test firings. Approximately 96,000 acres within Lake Erie and 1,427.75 acres of adjacent lands (wetlands, beach and dry land) are classified as formerly used target areas. The currently maintained impact/safety zone used by Camp Perry includes approximately 36,033 acres of the FUDS Lake impact zone (ESTCP, 2006).

The former Erie Army Depot was formerly used for artillery testing, resulting in impact areas on land, in Lake Erie, and in the channel, marshlands and beaches of the Toussaint River where it fronts the former Depot. The designated study site for the HeliMag demonstration encompasses 3,300 acres (see Figure 1) of the overall 50,000 acre area. This study site includes the FUDS beach from just northwest of the Toussaint River, south to Camp Perry, and the beaches and near-shore areas at the mouth of the Toussaint River.

The physiographic character and known munitions-use history of the study area are discussed in some detail in the ESTCP Demonstration Plan for this site (ESTCP, 2006) and in the technical report of previous MEC assessments at the site (Pope et al., 1996). The site characteristics most relevant to the HeliMag technology demonstration are described briefly below.

Topography and Soils. The study area is located along the south shore of the western basin of Lake Erie. The land is a low, flat, broad plain of sands deposited on top of older lake clays. The beach is a narrow, shallow depth, sandy barrier which includes wash-over deposits and evidence of breaching. The FUDS shore has a history of rapid erosion and retreat. Rubble-mound revetments have been installed as shore protection at the southeastern end of the study site through the Camp Perry boundary and fronting approximately 0.8 km (0.5 mile) of the central beach (Figure 5). Beach width varies from no dry beach zone up to approximately 150 m (500 feet).

Terrestrial Vegetation. The back beach area consists of areas of thickly vegetated marshlands within an open water channel and lagoon complex; scrub and woodlands exist in many areas as well. The trees extend in many areas close to the water line, which limited the shoreline area for helicopter surveys (Figure 6).

Aquatic Environment. Water levels in the study site respond to normal annual fluctuations in Lake Erie. The ESTCP Demonstration Plan notes that the western end of Lake Erie is shallow and subject to rapid water level fluctuations as storms and frontal passages can seiche (form a standing wave) both the local and entire lake water surface. Lake Erie is particularly prone to wind-caused seiches due to its elongated shape and shallowness. The survey area is comprised of shallow water areas only (limited to a few feet in depth). Storms causing wind-caused seiches would preclude surveys of the near shore areas due to fluctuation in water levels and winds.

Climate and Hydrology. Changeable weather conditions are common in the Lake Erie region, especially in the spring and fall. The Great Lakes have an influence the climate of the region by acting as a heat sink. The lakes moderate the temperatures of the surrounding land, cooling the summers and warming the winters. The lakes also act as a giant humidifier, increasing the moisture content of the air throughout the year. In the winter, this moisture condenses as snow when it reaches the land, creating heavy “lake effect” snowfall on the downwind shores of the lakes in some areas. Ice frequently covers Lake Erie. However, since demonstration was conducted mid-August, it was not expected that climate would limit the ability of the technology to survey the area.

Land Use. Multiple land uses occur within and near the study site. Along the northwest shore of the Toussaint River is a section of the Navarre Division of the Ottawa National Wildlife Refuge and the Davis-Besse Nuclear Power Station. The power station required aircraft information for the survey areas in its vicinity. In addition, a privately owned hunt club, The Toussaint Shooting Club, is located in the northwest portion of the marshlands. Last, the range fan for Camp Perry extends into the survey area; Camp Perry agreed to allow surveying in this area from September 11th to the 15th. The southwestern portion of the marsh contains a portion of the former Erie Army Depot, which is now the Erie Industrial Park; most of the buildings in the industrial park

are used for light commercial and storage purposes. However, the most lake-ward complex, which incorporates the original Erie Army Depot firing bunkers, is owned by ARES, Inc., which operates a commercial artillery and armament test facility. Both ARES and Camp Perry continue to use portions of the FUDS (both lake and marsh) for ordnance testing purposes.



Figure 5. Erosion prevention measures along shoreline.



Figure 6. Terrestrial vegetation.

3.4. Pre-Demonstration Testing and Analysis

Helicopter magnetometry technology has been fully evaluated by DoD through ESTCP. As a WAA tool, the NRL MTADS has been previously demonstrated at other WAA-PP sites, including: Kirtland Precision Bombing Range, New Mexico; Victorville Precision Bombing Range, California; and Pueblo Precision Bombing Range, Colorado. Additionally, Sky Research has begun deploying the updated helicopter-borne magnetometry sensor system to U.S. Air Force sites under the Air Force’s Military Munitions Response Program. To date, HeliMag data have been collected at Edwards Air Force Base, California, with four more Air Force sites scheduled throughout 2007.

Because the innovations by Sky Research changed both the platform and some of the technology components, the new HeliMag system was compared to the NRL MTADS system deployed on a Bell Long Ranger and previously demonstrated for the ESTCP WAA-PP before the new system was deployed to the Toussaint River site. The two systems have never been deployed over the same area. Therefore, data collected during high altitude flights in different areas and on different days were used to perform the comparison. In both cases, a 20 second section of data for comprehensive analysis was selected for the system comparison. The analysis showed that the Hughes /Sky DAS combination had a lower noise floor than the Bell/MTADS combination. The side-by-side comparison of the results of calibration lane flights demonstrating the two system’s capabilities was provided to ESTCP prior to mobilization (Appendix A).

Table 4 below summarizes the high altitude comparisons. Note that sensor 7 for the Sky system was malfunctioning and the noise floor of that sensor is not reported.

Table 4. Standard Deviations of the Bell Helicopter with NRL Data Acquisition Computer and the Hughes Helicopter with Sky DAS

	Raw NRL	Processed NRL	Raw Sky	Processed Sky
1	1.11	0.13	0.40	0.07
2	1.48	0.14	0.60	0.09
3	1.52	0.18	0.80	0.11
4	1.26	0.22	0.80	0.11
5	1.36	0.10	0.57	0.09
6	0.94	0.07	0.34	0.07
7	0.54	0.06	N/A	NA

3.5. Testing and Evaluation Plan

3.5.1. Demonstration Set-Up and Start-Up

Mobilization for this project required:

- 1) Mobilization of the equipment, pilot, and sensor operators.
- 2) Deployment of ground support personnel to establish ground fiducials, establish and operate GPS base stations, establish calibration line location and collect data on calibration location, and provide logistical support.
- 3) Establishment of calibration line and standard pre-collection maintenance and calibration procedures established during previous deployments.

A base of field operations was established at the Carl R. Keller Field, Port Clinton, OH, to provide fuel and temporary hanger/storage space during operations at the site. The methods to establish base station survey monuments, emplaced calibration items and ground targets appropriate for the sensors have been described in the demonstration plan for the former Pueblo Precision Bombing Range (Foley, 2005).

Ground Control

RTK GPS provided cm-accuracy real-time positioning and was used with the HeliMag system. It was also used to generate positions for ground fiducials and for positioning ground calibration data and field verifications. Sky Research employs an in-house professional land surveyor to assure that geospatial data generated by the project maintain accurate ties to the local coordinate system and to oversee the accurate field emplacement of fiducials for data registration and surrogate targets for sensor calibration and verification of classification and analysis algorithms.

Sensor Calibration Targets

A calibration line was established at the base of field operations at the airport. To confirm its suitability for the calibration line placement, background noise data was collected and reviewed before the calibration line was established. The calibration targets were placed on the ground surface at a spacing of 50 m at the orientations as listed in Table 5. Target positions were surveyed at two altitudes and the resulting signatures compared to calculated responses to confirm that the system is operating at its expected sensitivity. Calibration line surveys were conducted twice each day. No targets were buried and no attempt was made to measure a probability of detection.

Table 5. Emplaced Calibration Targets

Item	Depth	Orientation
8" steel cube	Ground level	
100 lb. bomb stimulant	Ground level	1 N-S 1 E-W
155 mm projectile	Ground level	1 N-S 1 E-W
2.75" warhead	Ground level	1 N-S 1 E-W

3.5.2. Period of Operation

Pre-planning for the survey was conducted in August of 2006, including submittal of the demonstration plan and final acceptance by the ESTCP Program Office. The ground surveys were conducted in August prior to mobilization of the ground crew and helicopter to the survey site. Mobilization of the helicopter from Ashland, Oregon, to Ohio began on September 5th, and the helicopter arrived on site on September 7th. The ground crew mobilized from Denver, Colorado, on September 6th and transported the fuel truck and equipment, arriving on site on September 7th. The sensor boom assembly, calibration lane construction and test flights were conducted on September 8th.

Surveys began on September 9th. The initial area surveyed was within the Camp Perry exclusion area because of the Camp Perry cooperation in suspending activities in this area for one week; re-flies were conducted in this area on September 15th to ensure data quality for the exclusion area. Surveying continued through the morning of September 16th; on the morning of the 16th, the survey ended when pilot error caused an accident which destroyed the helicopter, booms, and much of the electronic equipment. While the helicopter suffered significant structural damage, the pilot and sensor operator escaped without injury. A summary of the acres per day productivity prior to the 16th is provided in Table 6.

Table 6. HeliMag Data Collection Acreage

Data Collection Day	Acres Surveyed
September 9, 2006	400
September 10, 2006	500
September 11, 2006	517
September 12, 2006	494
September 13, 2006	708
September 14, 2006	659
September 15, 2006	111
Acres Collected	3,389 acres
Average Daily Productivity	484 acres/day

3.5.3. Operating Parameters for the Technology

Sky Research deployed the airborne MTADS system on the MD530 helicopter platform, together with pilot, system operator and ground support team to operate the RTK GPS base stations. The system uses an array of seven full-field Cs vapor magnetometers deployed on a 9 m boom mounted transversely on the front of the helicopter skids. The helicopter is typically flown at a low altitude (1.5 - 5 m), with a forward velocity of 15 – 20 m/s. The sensor boom extends well in front of the helicopter and is clearly visible to the pilot, which is important for these very low flight altitudes.

With the sensor spacing of 1.5 m, a data collection rate of 100 Hz, and a speed over ground of 20 m/s, the resulting data density provides 50 data points on a typical target to fit the dipole signature. Magnitude data points are merged with GPS positioning data to generate geo-referenced point data that are interpolated into magnetic surface maps, and analyzed for target picking and characterization.

Airborne MTADS

- 7 Cs vapor full-field magnetometers
- 1.5 m spacing on 9 m boom
- along-track data density: 15-20 cm typical

Ground Support

- RTK GPS base stations w/ radio link

Positioning and geo-referencing

- RTK GPS

Processing

- Custom DAS merging and point file creation
- UXOLab for initial surface interpolation
- UXOLab for target picking and classification
- ArcGIS for final interpolation and mosaicing, mapping, presentation
- ArcSDE/Sky Research Geophysical Data Center for storage and management

Flight Speed

- 15-20 m/s (30-40 kts)

Altitude

- 1.5-3 m AGL

Spatial Accuracy

- < 5 cm RMSE

3.5.4. Data Processing

Data processing was completed nightly following data collection survey. Data were downloaded via zip disks and uploaded via the Internet after each survey mission. Data processing was performed using custom application software running under the UXOLab geophysical data processing environment. An overview of this process is outlined in the flow chart below (Figure 7).

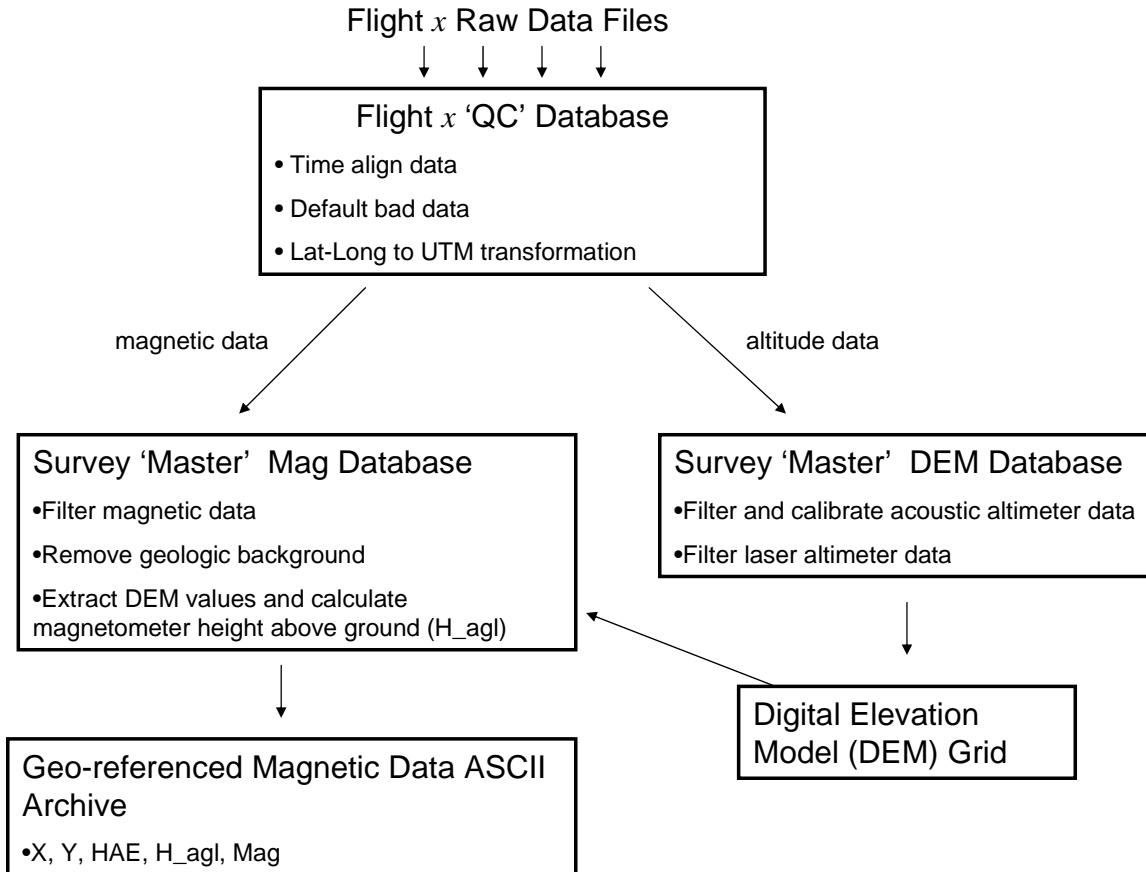


Figure 7. Helicopter MTADS processing flow chart.

During the first data processing stage, the raw data for a given survey flight were time-aligned and transcribed from the various raw data files into a 'flight' database. Routines were run to automatically reject or 'default' invalid data. Data were rejected based upon status flags present in the raw data records or, in the case of the magnetometer data, a simple 'in range' test may be used. The GPS geographic position coordinates were transformed to WGS84 UTM coordinates. At this point the data were visually inspected to ensure both integrity and quality. This pre-processing stage is instrumentation-specific and the steps required to transcribe these data into a

time-aligned database were dictated by the structure of the data outputs from each device and the manner in which they were logged. All data outputs were received by the on-board DAS. A time stamp was appended to each sample data string and the sample was then stored in a separate data file for each device. Table 7 provides a list of the raw data input files generated.

Table 7. Helicopter MTADS Raw Data Input Files

Device	Sample Rate (Hz)	Data Type	Filename extension	Remarks
Geometrics Model 822A Cs Magnetometers	400	RS232-ASCII	M19yyddd1A.sen M19yyddd2A.sen M19yyddd3A.sen...	A separate file is created for each of 7 magnetometers. The 400 Hz data are low-pass filtered and de-sampled to 100 Hz.
Trimble Model MS750 GPS position/attitude data	20/10	RS232-ASCII	P13yydddA.pos	Position data are in Trimble GJK message format, azimuth and roll are in Trimble AVR message format.
Trimble Model MS750 GPS time tag	1	RS232-ASCII	T14yydddA.time	Used to resolve the integer ambiguity of the GPS PPS signal in real-time – only stored for diagnostic purposes.
Optech Model 60 Laser Altimeter	10	RS232-ASCII	A15yydddA.alt	Measures helicopter height AGL.
Acoustic altimeters	10	Analog voltage	D22yyddd1A.dst	Measures sensor array height AGL at two points.

An important consideration for integration of the positioning system with geophysical sensors is that of time alignment. For dynamic applications, the time of applicability (TOA) of the geophysical sensor data must be aligned with the TOA of the measured positioning data to within one millisecond. Any measurement will have some latency before the data are collected and stored, which may be static or variable in nature. In addition to this latency, conventional time stamping of RS232 data is not precise and can inject hundreds of milliseconds of additional delays. Thus, simply time stamping the positioning data as it is transmitted to the DAS does not ensure that the TOA of the positions can be precisely aligned with that of the geophysical data.

GPS systems commonly have an internal latency that is variable (i.e., the time between the applicability of a given measurement and the transmission of the derived position will vary) in addition to the serial port variability. To allow users to know precisely when a measurement applies, the data message is time stamped (i.e., the position solution is given in four dimensions; time, X, Y, and Z) to a very high degree of precision. This time-stamp is the precise TOA of the

GPS position and attitude data. In addition, GPS receivers also output a pulse per second (PPS) trigger at every precise integer second to provide a means to synchronize the DAS time with GPS time. The SKY DAS uses this timing pulse and the Universal Time Coordinated (UTC) time message from the Trimble receiver to align its internal clock to GPS time with a very high degree of precision. The counting of the magnetometer Larmor signals is performed by a counter-board that is fully integrated into the SKY DAS. This allows precise alignment of the TOA of the magnetometer data with respect to the DAS time base.

The processing steps used to derive a final geo-referenced data set and associated images were as follows:

- 1) The raw data are collected at a sample rate of 400 Hz. After application of a low-pass filter the data are de-sampled to 100 Hz. Each de-sampled magnetometer value and associated time stamp (UTC) are transcribed into a Geosoft database into appropriately named channels (e.g. Time, Mag1_raw, Mag2_raw, etc.).
- 2) Using the existing Time channel and the UTC time stamp in each GPS data record, the GPS position and orientation data are interpolated to each magnetometer record. As part of this process, the GPS master antenna positions are translated to that of each sensor based upon the aircraft geometry and attitude.
- 3) The DAS time channel and the DAS time field in the raw data files are used to interpolate the ancillary data for each magnetometer record. The ancillary data channels include the following: laser, four acoustic altimeter channels (two for each acoustic altimeter station to provide redundancy), and fluxgate X, Y, and Z components.
- 4) After the data are transcribed into a database, invalid data are defaulted to 'dummy' values. The magnetometer data are defaulted outside of a reasonable range and the GPS data are defaulted based upon the values of the two status flags.
- 5) Long wavelength magnetic features are removed from the data through the use of a de-trend filter. This filter combines an iterative de-median process with a running average to derive the long-wavelength components that are removed from the magnetic data. The filter parameters are dependent upon the local site geology and the aircraft survey altitude.
- 6) The final filtered, geo-referenced, magnetic data are used to create Geosoft grids using a 1 grid cell size. These grids are used as the basis for the target selection process.

3.5.5. Demobilization

The survey was terminated early due to an accident which destroyed the helicopter, booms and much of the electronic equipment. An effort was made to salvage any equipment that was not totally destroyed. All of the salvaged equipment and wreckage were removed from the site.

4. Performance Assessment

4.1. Data Calibration Results

4.1.1. Data Calibration

The data collected over each target from the calibration line passes that are assumed to be valid (i.e., target positions are stable and data positioning quality is good) were analyzed with the Sky Research UXOLab dipole fit algorithm. This analysis derives the parameters for a model dipole that best fits the observed data. These parameters include horizontal position, depth, size, and solid angle (i.e., the angle between the Earth’s magnetic field vector and that of the dipole model). The derived parameters were examined for accuracy, (determined as the average error or ‘bias’ where relevant), and repeatability (indicated by the standard deviation), presented in Table 8.

Table 8. Calibration Results for Calibration Lane Targets

Dipole Fit Parameter	Bias	Standard Deviation
Easting	-0.17 m	0.11 m
Northing	-0.19 m	0.07 m
Depth	0.10 m	0.19 m
Size	NA	0.012 m
Solid Angle	NA	3.7 °

Figure 8 shows the derived positions for each target relative to the ground truth supplied. The accuracy of these positions relative to the ground truth is well within the range expected for the MTADS system. The calibration lines were flown in an N-S direction, resulting in better precision in the Northing than in the Easting due to the difference in sample density (along-track sample density is 5 to 10 times higher than for across-track). This is consistent with our findings from earlier projects (Foley and Wright 2006). A significant component of the bias reported in Table 8 and reflected in the ‘Position Error’ data in Figure 8 (blue diamonds) is probably due to errors in the ground truth. The ground truth positions were not surveyed in after emplacement, due to the unexpected nature of the conclusion of the data collection (the reacquisition of ground truth position data was simply overlooked in the confusion related to salvage of the helicopter and equipment). The coordinates used for analysis were the planned target position coordinates. Errors of a few tens of centimeters would be expected between planned emplacement and actual emplacement.

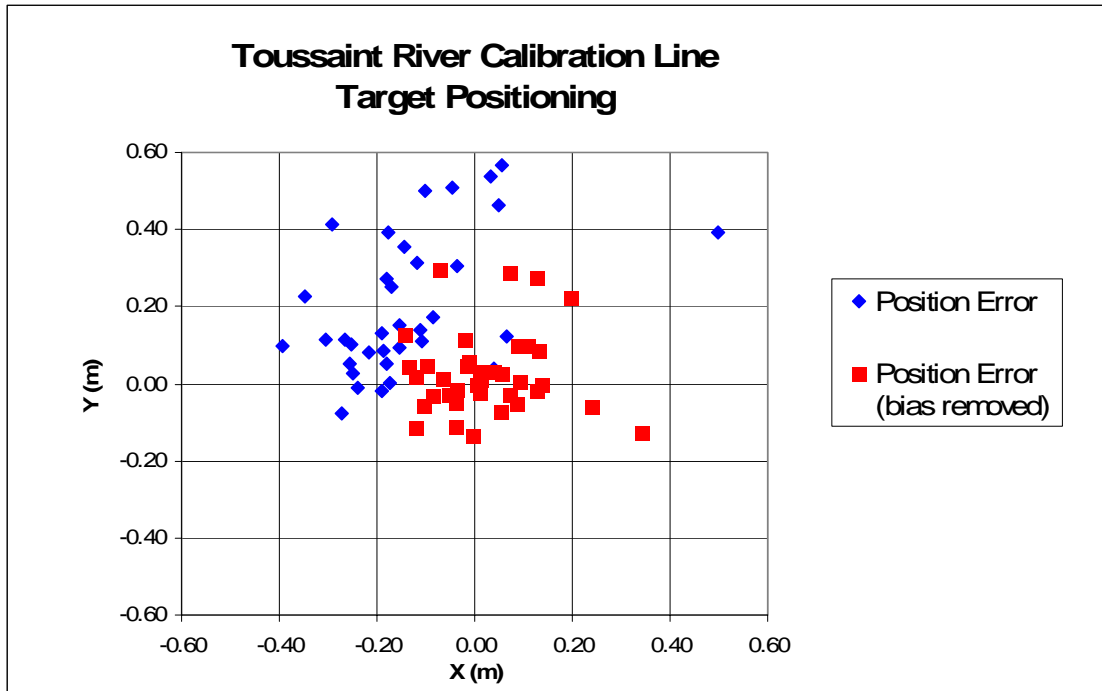


Figure 8. Calibration line target positioning errors.

4.1.2. Calibration Item Response

The dipole fit size estimate for any given munitions item will vary considerably depending upon the alignment of the object with the Earth's magnetic field. Therefore the size can only be used as a coarse estimate of the object size. For this reason, the accuracy of the size estimate of the calibration items is not of particular import when discussing the system performance, other than simply verifying that the estimate falls within the expected range for a given target. The size results for like items are relatively consistent with the exception of the 100 lb bombs. It appears that the difference in orientation of these two targets with respect to the earth's field has a large impact on the derived size of these targets. This finding is not inconsistent with the results shown in Billings et al. (2004). Because the calibration data consist of repeated flights over the same stationary targets, the repeatability of the derived size estimates demonstrates consistency in system performance (Figure 9).

In a manner similar to the size estimates discussed above, the dipole fit solid angle estimates depend heavily on the orientation of the target relative to the Earth's magnetic field. In the case of the calibration line test targets, the 'ground truth' is unknown and not really important. However the stability of this prediction for repeated flights over the calibration line is indicative of the performance of the airborne system (Figure 10).

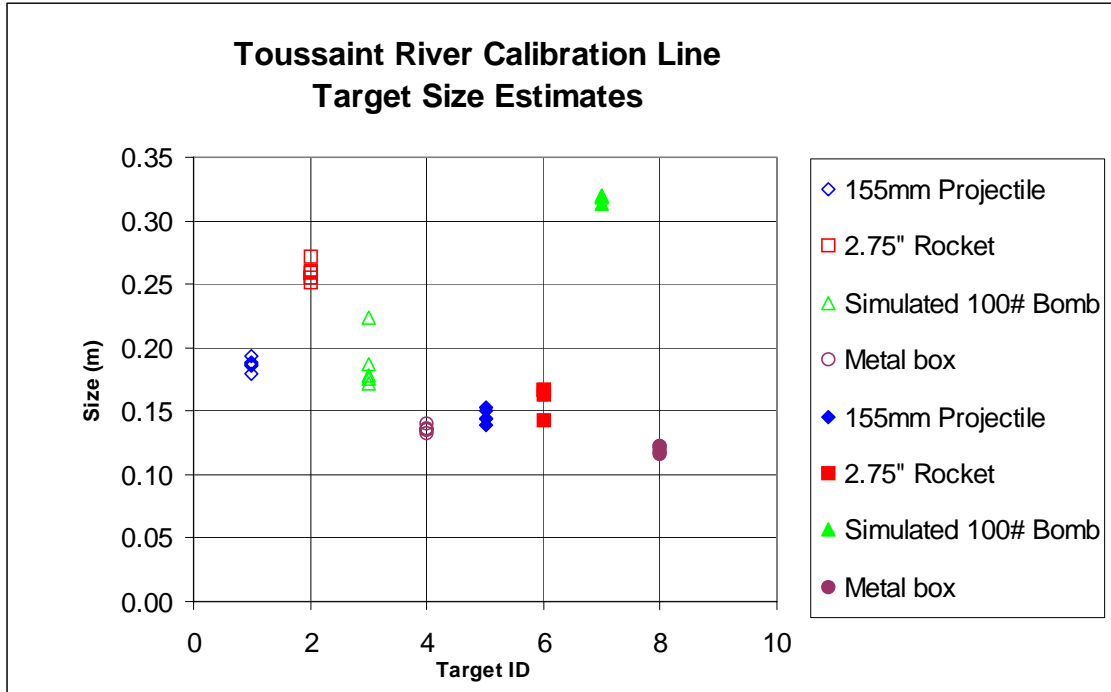


Figure 9. Dipole fit size estimates for calibration line targets.

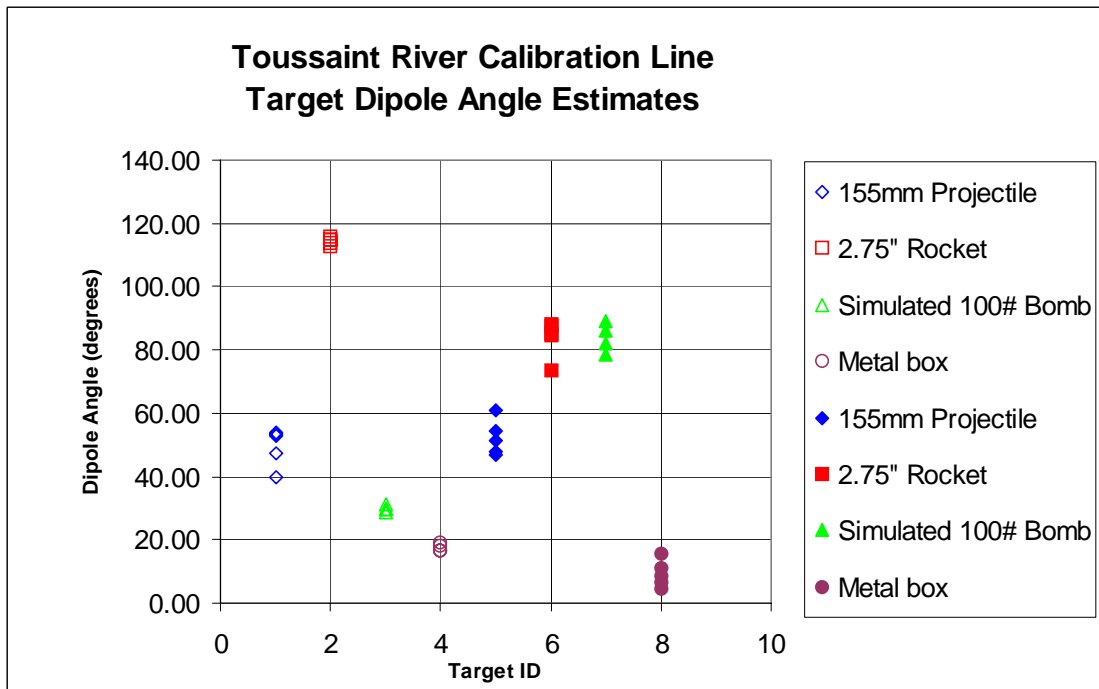


Figure 10. Dipole fit solid angle estimate for calibration line targets.

4.2. Anomaly Selection/Analysis

4.2.1. Anomaly Picking Methodology

For the purposes of WAA, the main goal is to delineate target density throughout the survey site. Target selection can be accomplished either manually or through automated routines; the geologic background signal largely determines what methods are best for a given site. Manual target selection is both subjective and labor intensive. The results obtained will vary considerably depending upon the skill level of the analyst; even an experienced analyst will find it difficult to be consistent with respect to his/her ability to select targets that are masked by geologic signal or overlapping signal from other targets. In areas of “quiet” geologic background, automatic target pickers can be faster to use, scientifically repeatable and more objective than manual target picking.

Automatic target pickers are not yet sophisticated enough to reliably detect closely spaced targets or targets that are at or below the same amplitude as local geologic signal. Where a reasonably experienced analyst is able to successfully discriminate a large number of targets from localized geologic signals that are of the same amplitude or higher, the automatic target detection routines that are currently available are not able to differentiate between our targets of interest and local geologic anomalies. As a result, automatic target selection routines must only be used to select targets with response amplitudes significantly above the nominal geologic noise; otherwise, an inordinate number of false targets are selected. Furthermore, the automatic routines do not perform well in areas of high target density.

In practice, the decision to pick manually, or use an auto-picker then add/reject targets manually is made based upon the number of targets to be picked and the extent of geologic/anthropologic clutter that must be dealt with. On this project there were relatively few anomalies and a significant number of anthropologic features. For this reason the decision was made to pick the targets manually.

At the Toussaint River site the distance of the sensor above potential targets was increased by the water depth. This resulted in significant reduction of anomaly amplitudes (particularly in deeper water) and a corresponding reduction in signal to noise of the targets. As a result, manual target selection was required because the automatic target pickers do not perform well on low signal to noise targets.

4.2.2. Anomaly Picking Results

Using manual picking procedures, 1,904 anomalies were selected from the data to assess the distribution of metal objects across the study area. Figure 11 illustrates the locations of these anomalies and their densities over the WAA study area.

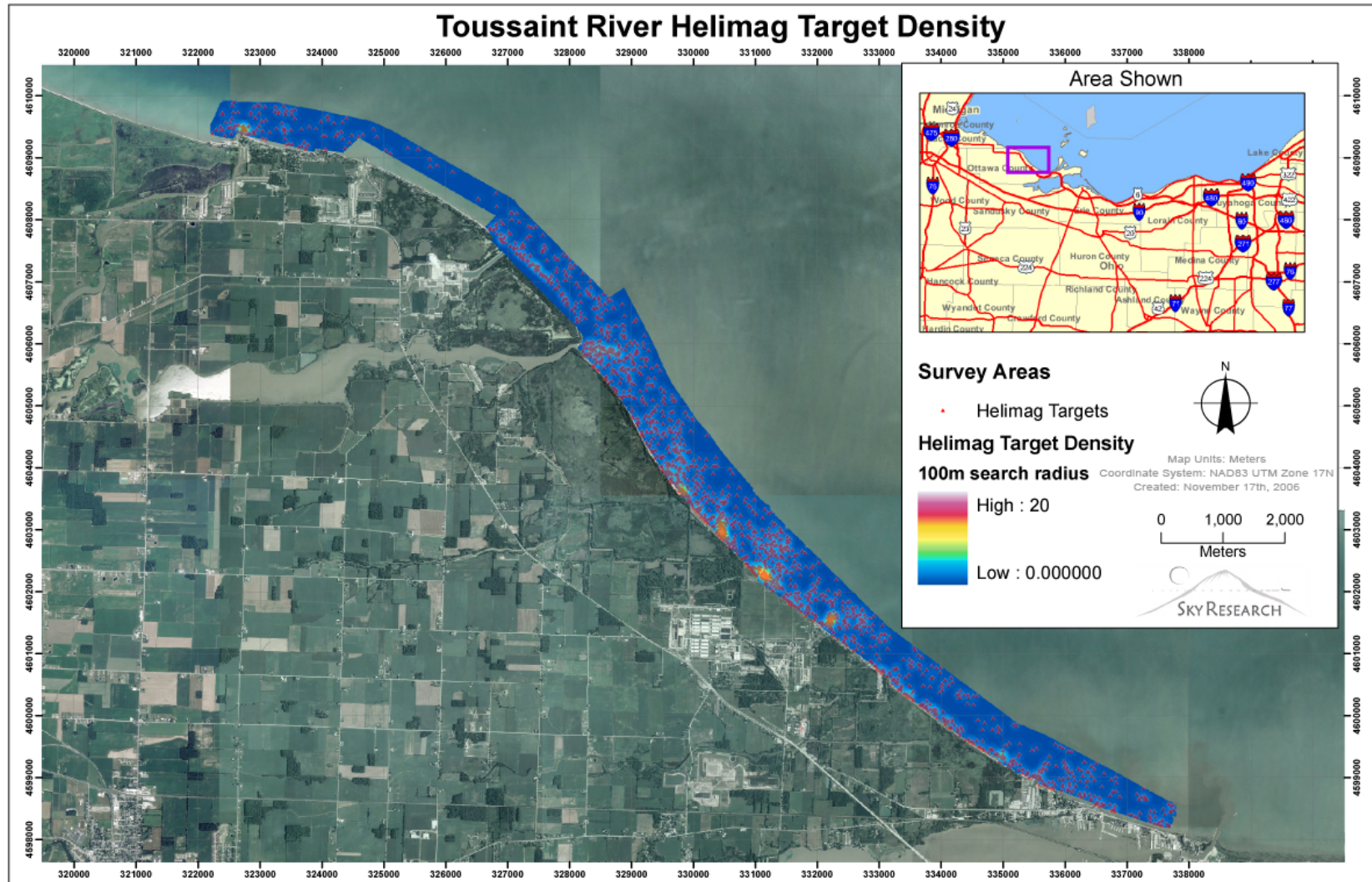


Figure 11. Target anomalies selected within the survey area and their densities.

4.2.3. Metal Density Analysis

To visualize the distribution of metal objects across the study area, a density raster was computed using a 75 m radius neighborhood kernel that assigned anomaly densities in anomalies per hectare to each cell in the raster. Simply described, at grid nodes of every two meters the number of targets that appear within a 100 m search radius were counted. This search radius provides the density in targets per 31,416 m². These values were then ‘normalized’ by dividing by 3.1416 to provide density estimates in targets/hectare. The resulting data were gridded to provide anomaly density images.

Our ability to detect objects of a given size is dependent upon our survey altitude above the object. In terrestrial surveys the measured survey altitude can be used to support assumptions about the size/depth of detectable targets. For example, based upon Figure 12 we expect to see all 155 projectiles (no remanent magnetic signal) down to a depth of 2.5 m. However, when flying over water we must be cognizant of the fact that the survey altitude above the lake bottom is not known. Therefore any assumptions regarding the minimum size of detectable targets can only be crudely estimated.

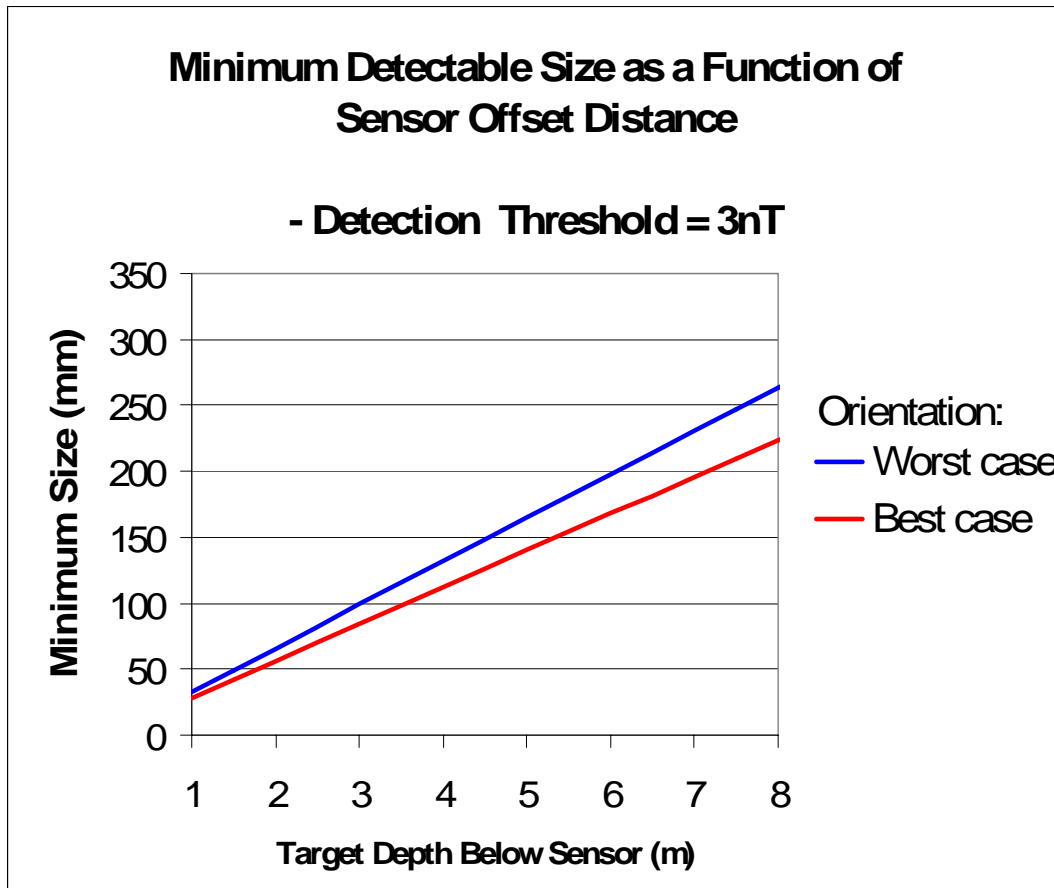


Figure 12. Minimum detectable ordnance size as a function of the separation distance between the sensor and the target. This distance is the sum of the sensor altitude above water, water depth and burial depth below the lake bed.

As a result of the increasing water depth, the target density estimates are skewed to show lower target densities as the water gets deeper. The relative densities moving along the shore line or, more accurately, along lines of equivalent depths will be valid. Additionally, we can assume that the predicted density of targets as large as 155 mm targets will be valid to water depths of 1 -2 m.

4.2.4. Target Dipole-Fit Analyses

Each selected anomaly was analyzed using the same dipole fit analysis described in Section 4.1.1. The fit results are provided in a spreadsheet called “Toussaint_R_Dipole_Fit_Results.xls”. Of the 1,904 selected targets, 1,155 were successfully fit to a dipole model. The lack of success in fitting the remaining targets is attributed to low signal to noise for these targets. The distribution of size estimates derived from these analyses is shown in Figure 13. There is a conspicuous absence of targets smaller than 150 mm. This is attributed to the increased target stand-off distance relative to previous terrestrial airborne surveys. We assume that the smaller targets had insufficient signal to be successfully fit to a dipole model.

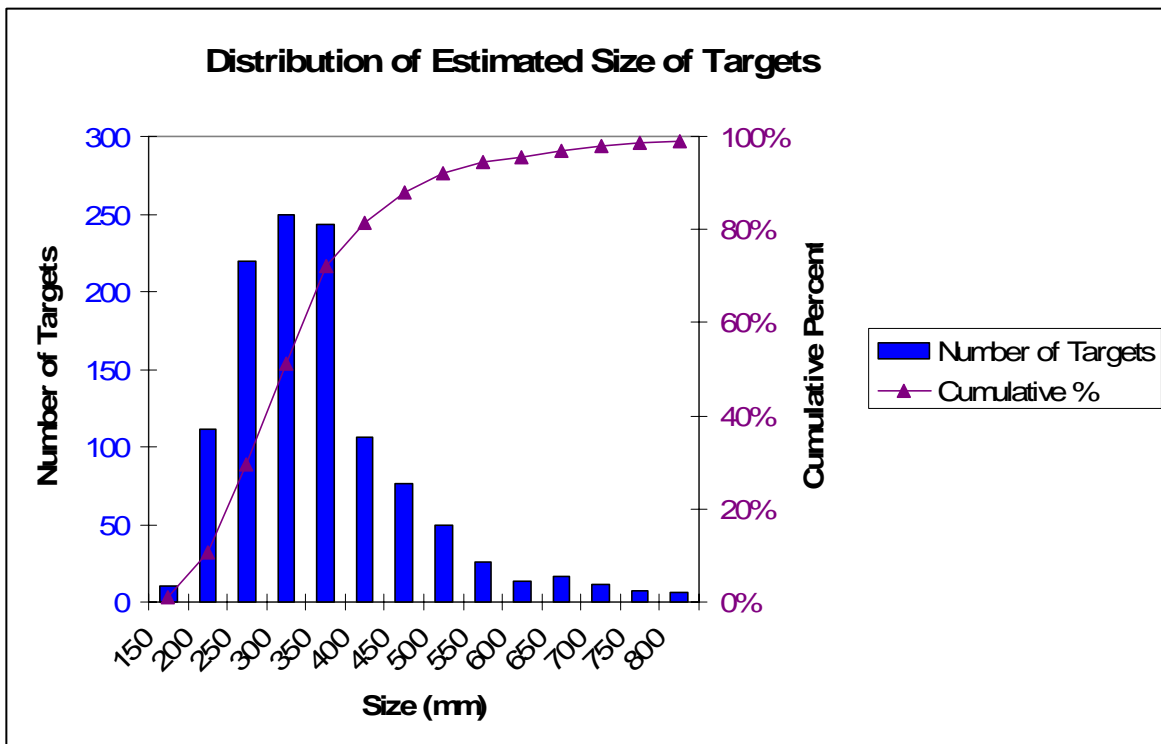


Figure 13. Distribution of dipole fit size estimates.

4.2.5. Intrusive Investigation Results

A small number of targets were selected for remediation to supply ground truth that could be used to ‘calibrate’ the results of the dipole fit analyses. These results are presented in tabular format in Appendix B and include 18 targets selected for investigation, summarized as follows:

- 7 x 155 mm projectiles
- 2 x 2.75 inch rockets
- 4 x non-UXO related objects
- 2 x objects buried in the lake bottom too deep to identify
- 3 x ‘no-contact’

The three ‘no-contacts’ were all located in very shallow water (0.25 m or less) making them susceptible to being moved by wave action or people in the time between the survey and the intrusive investigation. Of the seven 155 mm targets, only two were fit to a size that we would expect for this type of ordnance. The remaining five were all fit to a size that is significantly greater than we would expect. We attribute this phenomenon to the presence of significant remanent magnetization of these targets. In Figure 14 we present the recovered moments for these targets. Targets 1, 4, 5 and 6 exhibit significant rotation of their moments relative to the Earth’s field. This and the variability on the magnitude of these moments support the contention that a large part of the magnetic response of these targets is due to remanent magnetization. This evidence is consistent with earlier unverified reports of ordnance being put into the lake by means other than test firing.

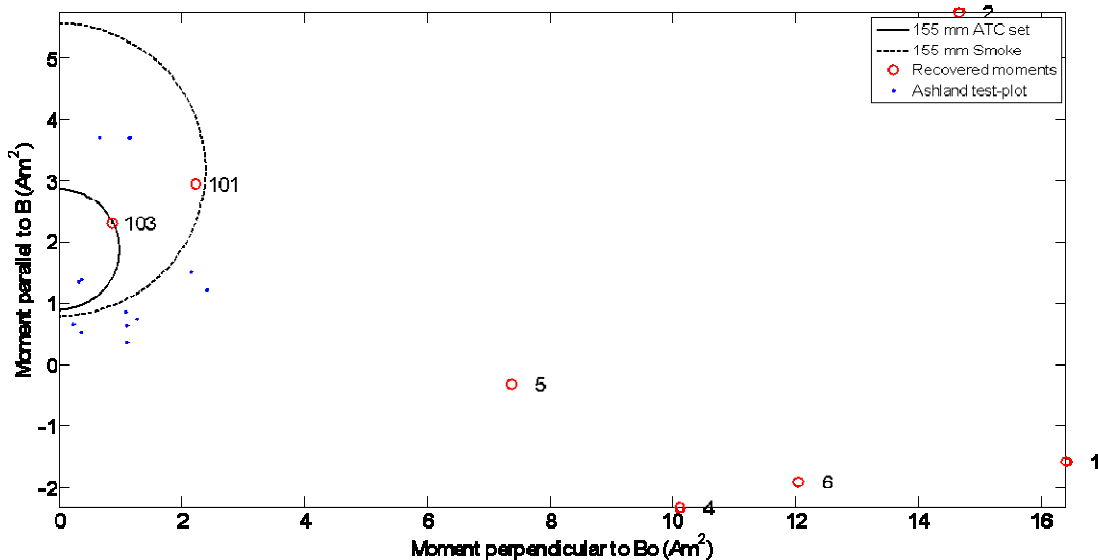


Figure 14. Recovered moments of 155 mm targets identified during the intrusive investigation. The moment vectors are plotted as their parallel and orthogonal components relative to the Earth’s field. The black circles represent expected results for two types of 155 mm projectiles.

If we factor in a significantly increased expected size for 155 mm projectiles, we can use the fit size distribution presented in Section 4.2.4 to assume that a very large percentage of the targets detected represent ordnance. This is also supported by the results of the intrusive investigation.

4.3. Performance Criteria

The performance of the helicopter magnetometry technology was measured against the criteria listed in Table 9.

Table 9. Performance Criteria for the Toussaint River HeliMag Technology Demonstration

Performance Criteria	Description	Type of Performance Objective
Technology Usage	Ease of use and efficiency of operations.	Primary/ Qualitative
Geo-reference position accuracy	Comparison of calibration target dipole fit analysis position estimates (in 3 dimensions) to ground truth.	Primary/ Quantitative
HeliMag survey area coverage	Percentage of survey area coverage surveyed.	Secondary/ Quantitative
Operating parameters (altitude, speed, overlap, production level)	Valued to be calculated and using average and mean statistical methods to compute each parameter.	Secondary/ Quantitative
System Noise	Accumulation of noise from sensors and sensor platforms, including GPS, rotor noise, radio frequencies, etc. calculated as the standard deviation of a 20 second window of processed data collected out of ground effect.	Primary/ Quantitative
Data density/point spacing.	(# of sensor readings/second)/ airspeed	Secondary/ Quantitative
MEC parameter estimates	The size and dipole angle estimates of the calibration items are consistent.	Secondary/ Quantitative

4.4. Performance Confirmation Methods

Table 10 details the confirmation methods that were used for each criterion, the expected performance and the performance achieved.

In light of the helicopter accident, claiming ‘pass’ for the ease of use criteria requires some explanation. It is Sky Research’s contention that the accident is an isolated event and should not be used in our evaluation of the ease of use criteria. This contention does not deny the seriousness of this incident nor the imperative requirement to take any and all reasonable

measures to prevent a recurrence of this type of incident. However in the context of this report, we do not feel it is appropriate to factor this incident into our performance assessment.

Position accuracy on a dynamic platform is very difficult to measure precisely. We are able to infer the position accuracy of the sensor data by using the position estimates derived from dipole fit analysis of data collected over known targets. Although there are additional error sources (other than just those due to the data positioning) in the dipole fit results, they are almost negligible due to the stability of the magnetometer calibration and the robustness of the dipole fit process. Because reciprocal passes will tend to hide along-track position errors (due to the robustness of the dipole fit process), the dipole fit analyses were performed on a single pass over the targets. The results for these analyses are presented in Table 8.

The spatial extent of a magnetic anomaly (from our targets of interest) is a factor of two times greater than the sensor offset distance. Based upon our minimum survey height of 1.5 m, we can conservatively define gaps in survey coverage as areas where the distance to the nearest sensor reading is greater than 2 m. Gaps in survey coverage are generally related to navigation (a combination of pilot skill, topography/vegetation, and wind conditions) or data integrity (primarily GPS fix quality). As a general practice, images representing the data from each day of survey flying are created to identify areas requiring fill-in flying to cover significant gaps in coverage. Invariably there will be a number of gaps in survey coverage that cannot be practically filled. To estimate the survey coverage performance, at every 0.25 m interval (grid node) we search through a 1 m radius for a valid data point. The number of grid nodes where valid data are found is divided by the total number of grid nodes to derive the percentage of survey coverage. Due to the helicopter accident, a portion of the original planned survey was not covered. In addition, re-flights to cover significant data gaps were not able to be performed. The un-surveyed area was excluded from the percent coverage calculation but the gaps where re-flights would normally have been flown were included, for a total of 3,388 acres covered and 63.4 acres not covered. Based upon these factors and acreages, the final coverage was 99.98%.

The assessment of the survey altitude and speed was performed by extracting a statistics for these parameters from the survey databases. Survey speed was consistently maintained between 15 and 25 kts, with some insignificant variation at the beginning or end of the survey lines. Survey altitude is a critical parameter for this type of investigation and is expected to be a little more variable than survey speed. In Figure 15, we present a histogram of the survey altitude performance. Prior to deriving these statistics, all altitudes above 5 m were rejected. These altitudes occur at the end of survey lines or during times when the helicopter has broken off a survey line and is circling back to reacquire it. The mean survey altitude was 2.0 m and the standard deviation was 0.51 m.

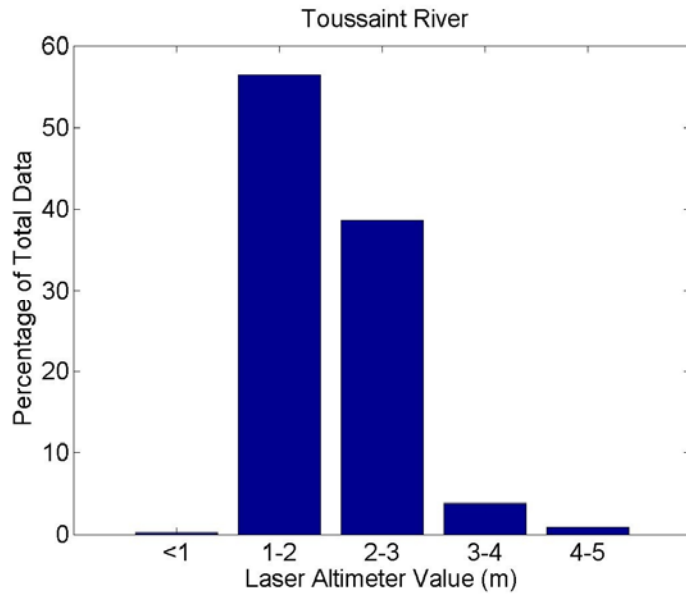


Figure 15. Histogram of sensor altitude above the water.

Prior to commencing survey operations, the HeliMag system was test flown to compare the base noise levels of the system to the NRL system. Details of this analysis are presented in Appendix A. The analysis showed that the Hughes 500/Sky DAS combination had an even lower noise floor than the Bell/AMTADS combination. In addition, the most significant noise source in the Bell helicopter was from the rotor at a frequency of 6.5 Hz while for the Hughes this frequency increased to 8 Hz. This provides a greater separation in frequency between the rotor noise and that of the anomalies of interest (which lie at lower frequencies), thus simplifying the noise filtering process.

The cross-track data density is essentially static and is a function of the system geometry. With the exception of isolated data gaps (addressed above) the ‘worst case’ spacing is our sensor spacing of 1.5 m. The effective density is much higher than this due to the significant overlap required to ensure (or at least minimize) data gaps due to the inevitable cross-track variation of the helicopter flight path. However, because the density is not uniform, we quote the ‘worst case’ as the data density achieved. Down-track data density is much higher than the cross-track density and is a function of survey speed. At our final sample rate of 100 Hz, the survey speeds of 8 – 13 m/s (15 – 25 kts) resulted in down-line data spacing of 0.08 - 0.13 m.

Table 10. Performance Metrics Confirmation Methods and Results

Performance Metric	Confirmation Method	Expected Performance	Performance Achieved
Technology Usage	Field experience using technology during demonstration	Relative ease of use	Pass
Geo-reference position accuracy	Infer sensor position accuracy from position estimates of calibration targets derived using dipole analysis of repeated data collection over calibration targets	Horizontal < 0.25m; Vertical < 0.5m	Horizontal 0.13 m; Vertical 0.16 m
HeliMag survey area coverage	Percentage of survey area coverage surveyed	95%	99.9%
Operating parameters (altitude, speed, overlap, production level)	Field data logs will be used to calculate the operating parameters	Altitude: 1-3 m AGL; Speed: 15-20 m/s (30-40 kts); Overlap: 10%; Production Level: 300 acres/day	Altitude: Mean 2.5 m AGL, stdev 0.55 m; Speed: 8-13 m/s (15-25 kts); Overlap: 37%; Production Level: 400 acres/day
System Noise	The system noise will be calculated as the standard deviation of a 20 sec window of processed high altitude data.	<1 nT	0.11 nT
Data density/point spacing.	Calculated based upon system sample rate and survey speed (along track) and system geometry and survey line spacing (cross track).	0.5 m along-track; 1.5 m cross track	0.08 – 0.13 m along track; 1.5 m cross track (max)
MEC parameter estimates	Comparison of analysis results of repeated data collected over calibration targets.	Size <0.02 m; Solid Angle < 10°	Size: 0.012 m; Solid Angle: 3.6°

5. Cost Assessment

5.1. Cost Reporting

Cost information associated with the demonstration of all airborne technology, as well as associated activities, were tracked and documented before, during, and after the demonstration to provide a basis for determination of the operational costs associated with this technology. For this demonstration, Table 11 contains the cost elements that were tracked and documented for this demonstration. These costs include both operational and capital costs associated with system design and construction; salary and travel costs for support staff; subcontract costs associated with airborne services, support personnel, and leased equipment; costs associated with the processing, analysis, comparison, and interpretation of airborne results generated by this demonstration. The cost of the magnetometers used for the HeliMag technology were used through a CRADA with NRL; as such, the actual cost of using the technology was not captured in this demonstration. However, we will estimate the true cost of using this technology, in addition to the cost and performance of all technologies demonstrated, in the ESTCP Cost and Performance Report submitted following this demonstration. In addition, due to the helicopter incident, the cost of demobilizing the helicopter is not included in the cost reporting. This cost would increase the cost per acre analysis.

Table 11. Cost Tracking

Cost Category	Sub Category	Details	Costs (\$)
Start-Up Costs	Pre-Deployment and Planning	Includes planning, contracting, site visit and site inspection	\$26,917
	Mobilization	Personnel mobilization, equipment mobilization, and transportation	\$45,917
Operating Costs	Helicopter Survey	Data acquisition and associated tasks, including 58 hours of helicopter operation time	\$135,841
Demobilization	Demobilization	Demobilization, packing, calibration line removal	\$23,496
Data Processing and Analysis	Data Processing	Initial and secondary processing of data	\$29,414
	Data Analysis	Analysis of airborne magnetometry datasets	\$13,438
Management	Management and Reporting	Project related management, reporting and contracting	\$46,489
Total Costs			
Total Technology Cost			\$321,512
Acres Surveyed			3,388
Unit Cost			\$95/acre

5.2. Cost Analysis

The major cost driver for an airborne survey system is the cost of aircraft airtime. In terms of tasks, this constitutes a major percentage of the data acquisition costs—the single largest cost item. In addition, mobilization costs for the helicopter were significant. Generally, this is a function of distance from the home base for the aircraft, equipment and personnel. The demobilization costs reported above do not include the cost of the helicopter time due to the helicopter incident; otherwise, the cost would be expected to be \$22,412 higher. Data processing and analysis functions made up the bulk of the remaining costs.

Project management and reporting were a significant cost for this demonstration, as the project was conducted under the WAA-PP and required more meetings, travel and reporting than would generally be expected for a production level survey. Last, mobilization and demobilization was a significant task in terms of cost. Generally, this is a function of distance from the home base for the aircraft, equipment and personnel.

Costs associated with validation were not considered in the cost analysis, as the validation was conducted as part of the WAA-PP.

6. Implementation Issues

6.1. Regulatory and End-User Issues

The ESTCP Program Office has established a WAA-PP Advisory Group to facilitate interactions with the regulatory community and potential end-users of this technology. Members of the Advisory Group include representatives of the US EPA, State regulators, Corps of Engineers officials, and representatives from the services. ESTCP staff have worked with the Advisory Group to define goals for the WAA-PP and develop Project Quality Objectives. As the analyzed data from the demonstrations become available, the Advisory Group will assist in developing a validation plan.

There will be a number of issues to be overcome to allow implementation of WAA beyond the pilot program. Most central is the change in mindset that will be required if the goals of WAA extend from delineating target areas to collecting data that are useful in making decisions about areas where there is not indication of munitions use. A main challenge of the WAA-PP is to collect sufficient data and perform sufficient evaluation that the applicability of these technologies to uncontaminated land and their limitations are well understood and documented. Similarly, demonstrating that WAA data can be used to provide information on target areas regarding boundaries, density and types of munitions to be used for prioritization, cost estimation and planning will require that the error and uncertainties in these parameters are well documented in the program.

7. References

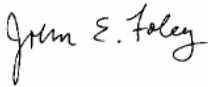
- Billings, S. D., 2004. Discrimination and classification of buried unexploded ordnance using magnetometry: *IEEE Transactions of Geoscience and Remote Sensing*, 42, 1242-1251.
- Billings, S.D., and F. Hermann, 2003. "Automatic detection of position and depth of potential UXO using a continuous wavelet transform", in *Proceedings of SPIE Vol. 5089, Detection and Remediation Technologies for Mines and Minelike Targets VII*, pp 1012-1022, 2003.
- ESTCP, 2006. "Demonstration Plan Former Erie Army Depot and Toussaint River", Draft.
- Foley, J. and D. Wright, 2005. "Wide Area Assessment Demonstration Plan for LiDAR, Orthophotography, Hyperspectral Imaging and Helicopter MTADS at Pueblo Precision Bombing Range #2", Sky Research.
- Foley, J. 2006. "Wide Area Assessment Demonstration Plan for Helicopter MTADS at Former Erie Army Depot and Toussaint River, OH", Sky Research.
- Foley, J. and D. Wright, 2006. "Wide Area Assessment Interim Report for Phases I and II LiDAR, Orthophotography, and Helicopter MTADS at Pueblo Precision Bombing Range #2", Sky Research.
- Nelson, H., J. McDonald and D. Wright, 2005. "Airborne UXO Surveys Using the MTADS," Naval Research Laboratory NRL/MR/6110--05-8874.
- Pope, J., Lewis, R. and T. Welp, 1996. "Beach and Underwater Occurrences of Ordnance at a Former Defense Site: Erie Army Depot, Ohio", Technical Report CERC-96-1, U.S. Army Corps of Engineers Waterways Experiment Station.
- Tuley, M. and E. Dieguez, "Analysis of Airborne Magnetometer Data from Tests at Isleta Pueblo, New Mexico", IDA Document D-3035, July 2005.

8. Points of Contact

Table 12. Points of Contact

Point of Contact	Organization	Phone/Fax/email	Role in Project
Dr. John Foley	Sky Research, Inc. 445 Dead Indian Road Ashland, OR 97520	(Tel) 978.479.9519 (Fax) 720.293.9666	Principal Investigator
Mr. David Wright	Sky Research, Inc. 445 Dead Indian Road Ashland, OR 97520	(Tel) 919.303.3532	Co-Principal Investigator
Ms. Stacey Kingsbury	Sky Research, Inc. 445 Dead Indian Road Ashland, OR 97520	(Tel) 540.961.9132 (Fax)	Project Manager
Mr. Jerry Hodgson	USACE Omaha District 215 N. 17 th Street Omaha, NE 68102-4978	(Tel) 402.221.7709 (Fax) 402.221.7838	Federal Advocate
Mr. Hollis (Jay) Bennett	US Army R&D Center (CEERD-EE-C) 3909 Halls Ferry Road Vicksburg, MS 39180-6199	(Tel) 601.634.3924	DoD Service Liaison

Project Lead Signature:



Appendix A: Comparison on NRL DAS with Bell and Sky Hardware DAS with Hughes 500

25 August 2006

Summary

As part of ESTCP-0535, Sky Research will deploy our HeliMag system to the Toussaint River demonstration site to collect approximately 3,300 acres of magnetometer data. Sky Research intends to use a Hughes 500 series helicopter and boom platform to collect data using our new hardware data acquisition system (Sky DAS). The ESTCP Program Office requested a comparison of the noise characteristics of this new HeliMag system versus that of the NRL AMTADS system previously deployed on Bell 206L series helicopters and demonstrated for the ESTCP Wide Area Assessment Pilot Program. Because site conditions and target response amplitudes are the same for each system, the relative efficacy of the systems may be evaluated by a comparison of their platform/helicopter related noise characteristics.

The two systems have never been deployed over the same area. Therefore, for this comparison we use data collected during high altitude flights in different areas and on different days. In both cases, we selected a 20 second section of data for comprehensive analysis. As the analysis reported here shows, the Hughes 500/Sky DAS combination has an even lower noise floor than the Bell/AMTADS combination. In addition, the most significant noise source in the Bell helicopter was from the rotor at a frequency of 6.5 Hz while for the Hughes this frequency is increased to 8 Hz. This provides a greater separation in frequency between the rotor noise and that of the anomalies of interest (which lie at lower frequencies), thus simplifying the noise filtering process. We also provide a comparison of the heading effects imposed by the static magnetic signature of each platform. These effects manifest themselves as maneuver noise in the raw magnetic data. For most UXO applications the response period of these effects is sufficiently long to allow them to be removed (along with gross geology and magnetic diurnal variations) using trend removal filters. However it is prudent to ensure that the static signature of the Hughes helicopter is not orders of magnitude greater than that of the Bell.

Table 1 summarizes the high altitude comparisons. Note that sensor 7 for the Sky system was malfunctioning and the noise floor of that sensor is not reported. See the text for a discussion of the raw noise in the Sky HeliMag as it is bimodal and hence the standard deviations listed below under the "Raw Sky" column may not be reliable.

Table 1. Standard deviations of the Bell helicopter with NRL DAS and the Hughes 500 with the Sky DAS

	Raw NRL	Processed NRL	Raw Sky	Processed Sky
1	1.11	0.13	0.40	0.07
2	1.48	0.14	0.60	0.09
3	1.52	0.18	0.80	0.11
4	1.26	0.22	0.80	0.11
5	1.36	0.10	0.57	0.09
6	0.94	0.07	0.34	0.07
7	0.54	0.06	NA	NA

NRL DAS and Bell Helicopter

A high altitude test flight of the Bell Long Ranger system with the NRL DAS was used for the analysis reported here. The raw and processed data were supplied by Mike Tuley of IDA. The data were imported into UXOLab and areas with steep turns were discarded (as the helicopter causes a strong heading dependant variation in the magnetic field). Line 6 in Figure 1 was selected for further analysis as this line had sections of data that were free of lower frequency variations in magnetic field (possibly caused by intentional yaw maneuvers from the pilot). The analysis reported below uses twenty seconds of data between GPS times 67195 and 67215 (Figure 2)

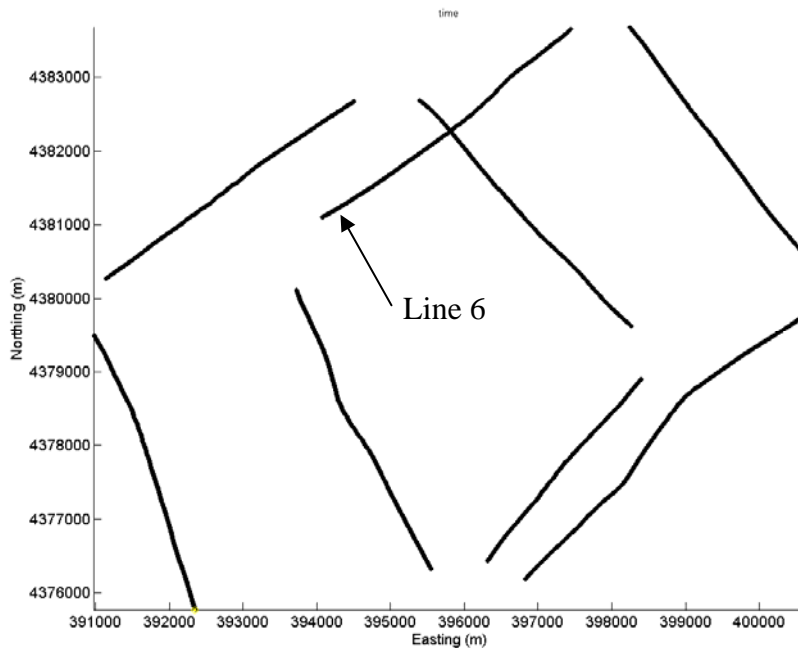


Figure 1: Plan view of the high altitude data available from the NRL AMTADS system on the Bell Long Ranger.

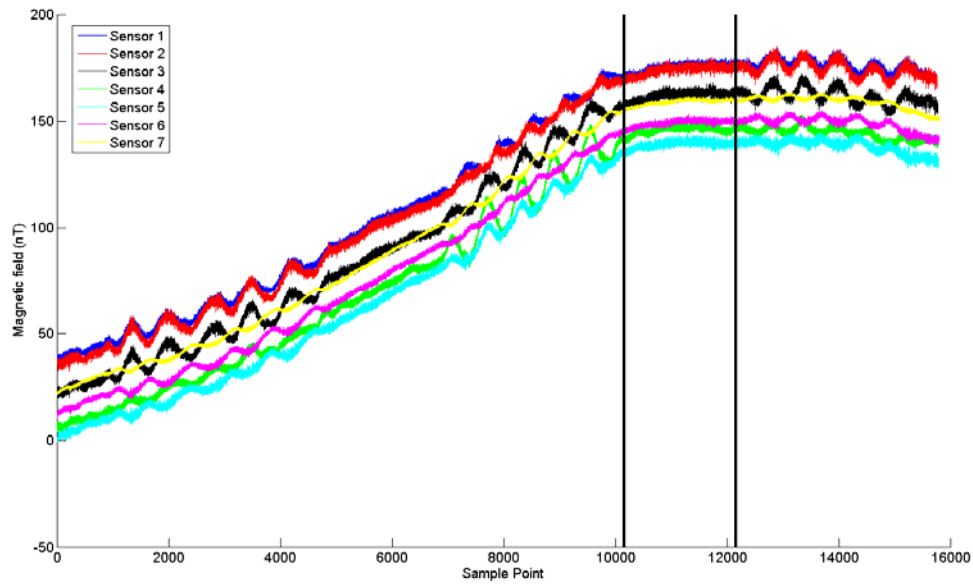


Figure 2 : Raw NRL data from the line selected for analysis.

The 20 seconds snippets of data for each sensor were demedian filtered to remove any trends in the data. The noise varies from sensor to sensor and is generally greatest for the middle sensor (sensor 4). A time-series of the raw and processed data for sensor 4 is shown in Figure 3. The raw data varies from about -2 to +2 nT. The standard deviation of the readings is 1.26 nT. For the processed data the variation is reduced by a factor of about 5-10, with a unimodal distribution and a standard deviation of 0.22 nT (Figures 3 and 4).

Figure 4 shows histograms of the raw and processed data for sensors 1 to 6. The histograms of the raw data are unimodal except for sensor 4. As explained in Appendix A the reason this distribution is bimodal is the dominant noise source due to the rotor noise at 6.5 Hz (Figure 5). This rotor noise is most significant on sensor 4 which is the closest sensor to the motor.

Note that the rotor noise at 6.5 Hz is not completely suppressed in the processed data for sensor 4 (Figure 5). The power spectrum was obtained by breaking the 2000 samples into 8 sections of 400 samples long. Each of these sections of data were multiplied with a window function (Kaiser-Bessel) and the FFT was calculated. The power-spectrums of each of the 8 sections were then averaged. This method for spectral estimation produces smoother and more reliable spectral estimates than the standard periodogram analysis used in the IDA report. However, note that the spectra estimated here and in that report correspond with the same peaks at 6.5, ~26, and 40 Hz and exhibit the same overall trends in the spectrum.

Helicopter System Comparison

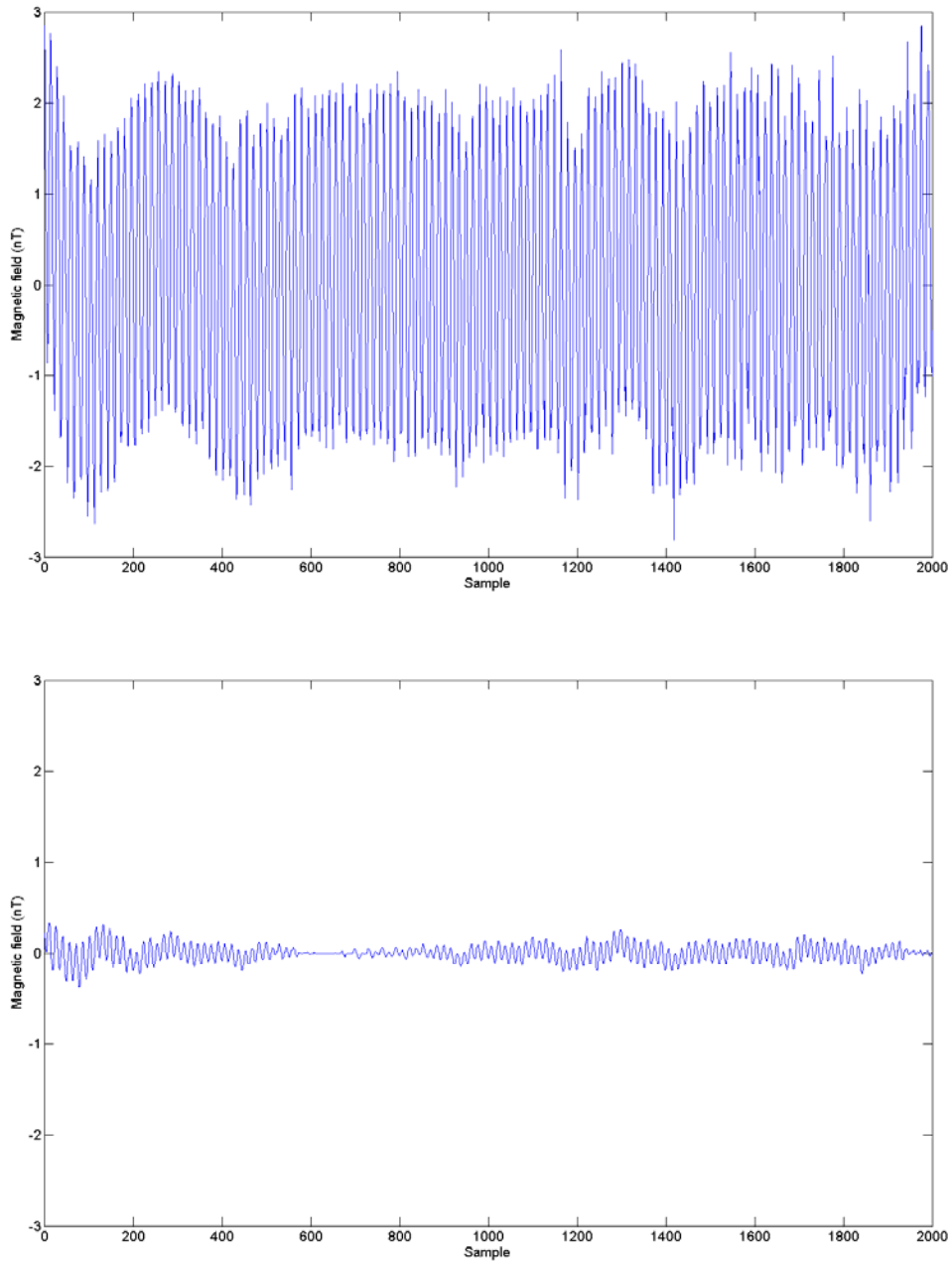


Figure 3: Detrend filtered data for sensor 4. The top row is minimally processed, the bottom row is after standard AMTADS noise filtering.

Helicopter System Comparison

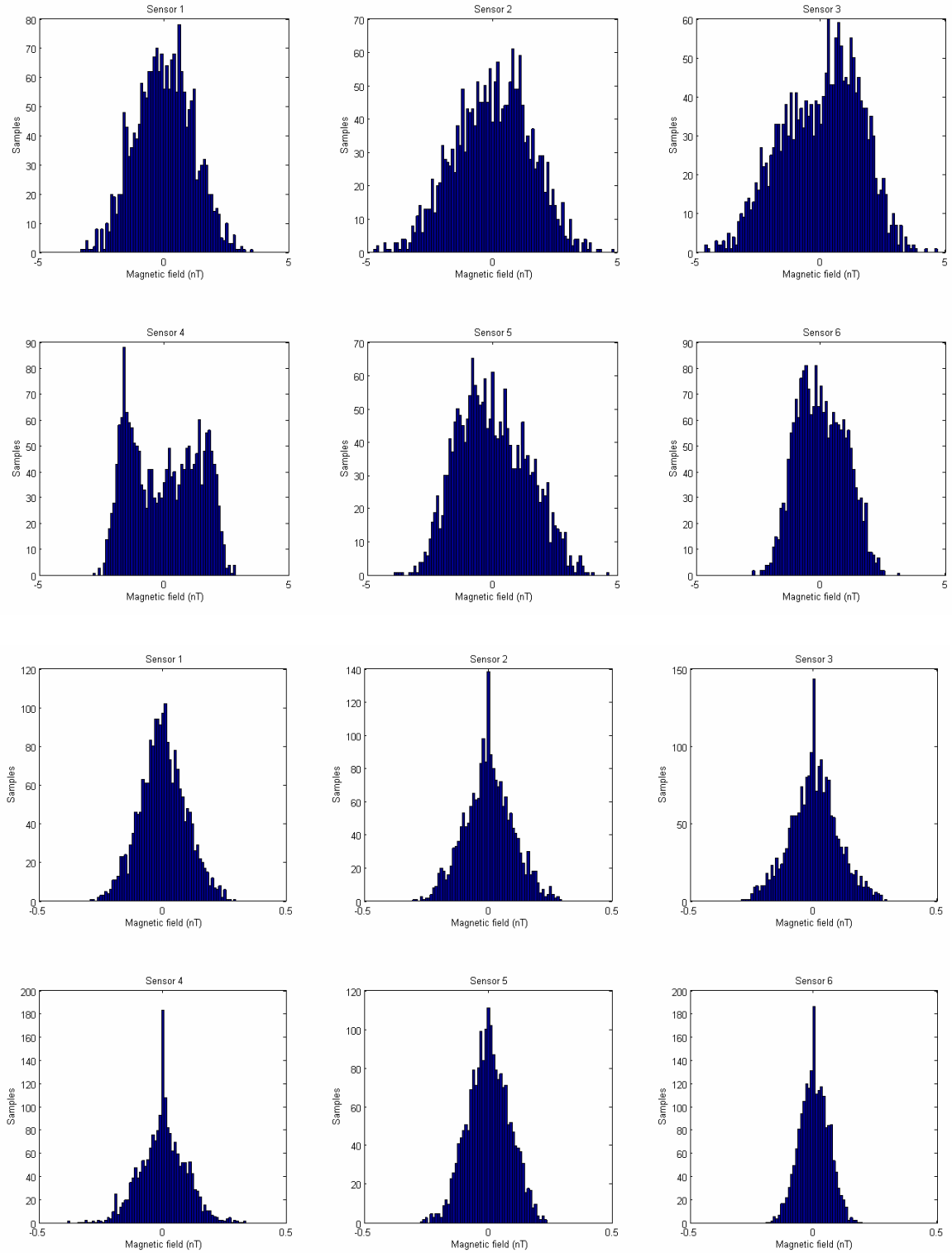


Figure 4: Histograms of the detrend filtered NRL data, with minimally processed on top and processed on bottom.

Helicopter System Comparison

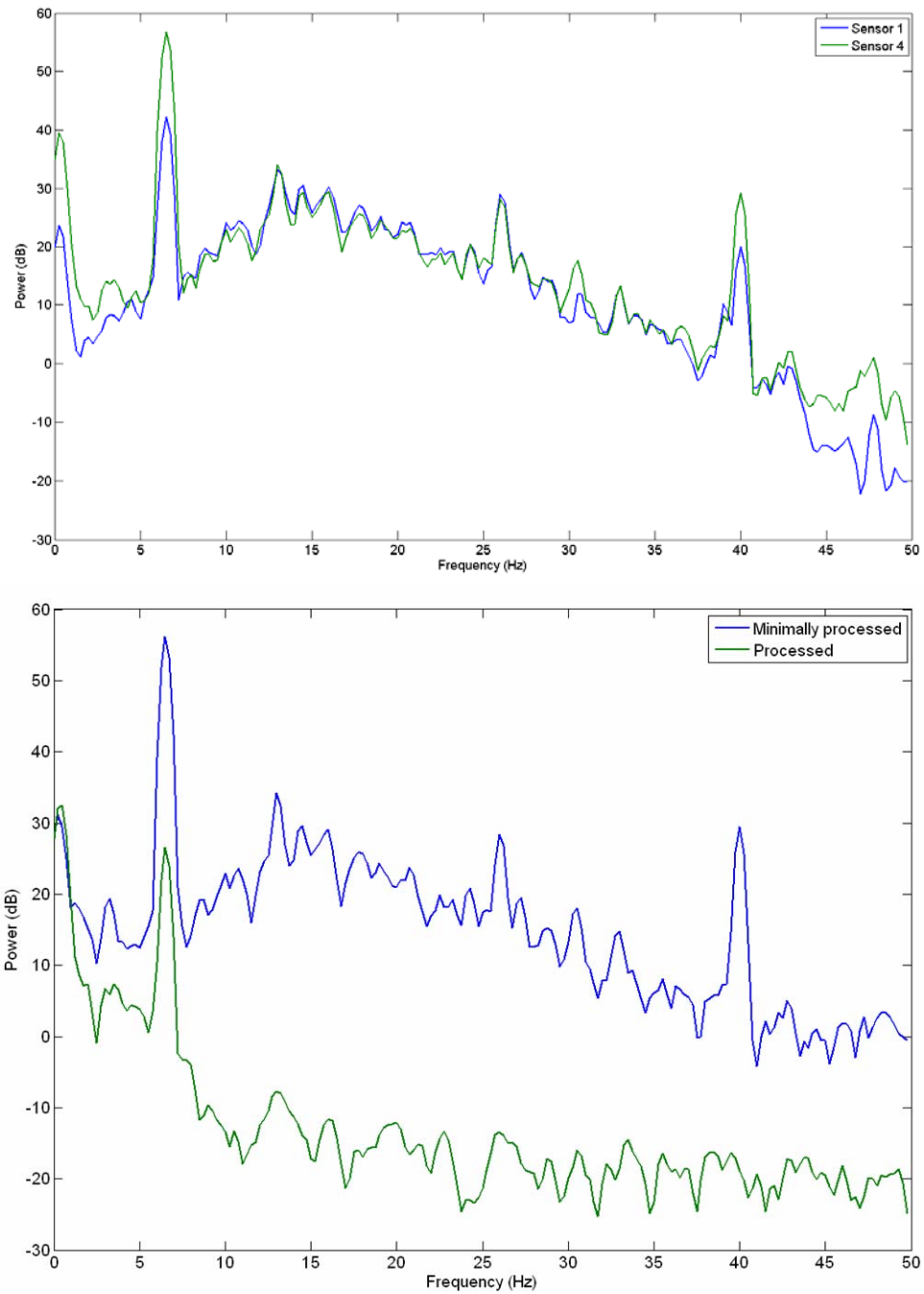


Figure 5: Top: Power spectrum of the raw data for sensors 1 and 4. Bottom: Power spectrum for sensor 4 of the raw and processed AMTADS/Bell system

The final aspect to consider is the effect of the heading of the helicopter on the magnetic field recorded by the sensors. As shown in previous demonstrations, heading (and pitch/roll) changes are slow enough that they do not interfere with the signals of the anomalies of interest. A simple moving median filter is able to suppress heading and diurnal changes in the Earth’s field. In Table 2, we compare the magnetic fields in at each sensor before and after 4 turns during the high altitude flights. These should provide an indication of the effect of heading on the field recorded by each sensor (although the magnetic field also varies spatially between the readings at different headings, so this estimation process is imperfect). Through a 180 degree change in direction, the field changes by about 60 nT (obtained as twice the average value in Table 2). In Figure 6, we plot the differences in the magnetic field at the 49 sensor intersections that occur where the flight path crosses. There is up to a 40 nT difference in recorded field at this location where the heading varies by 90 degrees (this just provides a second indication of the magnitude of the heading effect).

Table 2. Difference in the magnetic field at each sensor at the start and end of each of 6 turns

Heading before turn	Heading after turn	Heading change	Sensor 1 (nT)	Sensor 2 (nT)	Sensor 3 (nT)	Sensor 4 (nT)	Sensor 5 (nT)	Sensor 6 (nT)	Sensor 7 (nT)
134.2	-149.9	75.9	-4.5	1.4	9.8	9.7	-2.8	-12.0	-13.6
-108.7	-39.7	69.1	58.4	59.6	56.5	45.6	40.8	45.5	49.6
-13.2	46.1	59.3	-26.2	-33.7	-41.1	-42.7	-31.8	-24.1	-17.7
56.2	121.0	64.7	-16.8	-23.3	-17.2	4.0	15.0	12.5	8.4
		Avg.	26.5	29.5	31.2	25.5	22.6	23.5	22.3

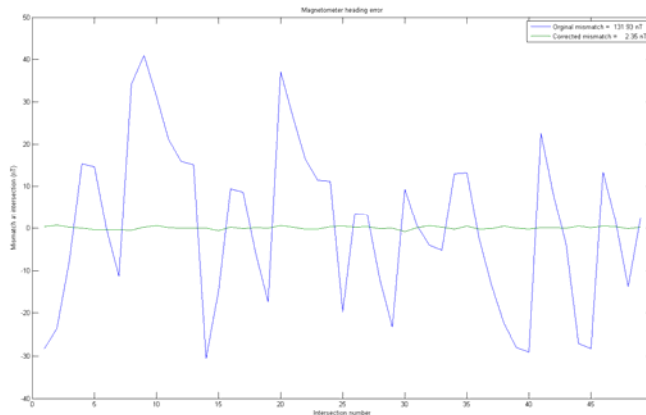


Figure 6: Differences in the magnetic field at the 49 sensor-sensor intersections where the flight-path crosses in Figure 1.

Sky Hardware DAS and Hughes 500 Helicopter

For the Hughes 500/Sky DAS system, we use high altitude data collected over the Ashland test plot on June 3, 2006 (Figure 7). We use 20 seconds of data from line 6 between GPS times 65624 and 65644 seconds (Figure 8). Note that sensor 7 was malfunctioning and data from it is not included here. The 400 Hz data were low-pass filtered with a 52 Hz cut-off frequency and downsampled to 100 Hz (equivalent to the low-pass filter and 100 Hz sample rate of the AMTADS). The data were detrend filtered and for each of the sensors the data are mostly contained within a +/- 1.5 nT range (Figure 9). Note that all histograms for these minimally processed data are bimodal, with the strongest effect evident with sensor 4 (closest to the rotor-hub presumably causing the noise). As explained in Appendix A, the bimodal distributions occurs because of the dominant sinusoidal noise source at 8 Hz (Figure 11). After applying a 7-9 Hz notch filter, the system noise is suppressed considerably and the distribution is unimodal (Figures 9 and 10). Table 1 provides standard deviations of the minimally processed and 7-9 Hz notch filtered data.

The dominant feature in the power spectrum (Figure 11) is the peak at 7-9 Hz. There are also other smaller peaks at 16, 20, 36 42 and 48 Hz, some of which are harmonics of the dominant peak. Comparing sensors 1 and 4, it is evident that the rotor noise and harmonics are more significant for sensor 4.

The final aspect to consider is the effect of the heading of the helicopter on the magnetic field recorded by the sensors. To investigate the effects of heading (but not pitch/roll) we analyze each intersection of each sensor with every other sensor in the high altitude flights (Figure 12). There are enough intersections with this flight path that we can fit a function of azimuth to each sensor and use that to predict the effect of heading (Figure 12). This analysis shows that for a full 360 rotation there will be a ~50 nT variation for sensor 1 rising to a maximum variation of ~120 nT for sensor 3, with all other sensors having values between 50 and 100 nT. It's difficult to directly compare the heading analysis for the Hughes and Bell helicopters as the flight plans were so difference (the Hughes flights had many flight-path intersections, the Bell only one, the Bell covered a much larger area and encountered spatial field variations on the order of 200 nT). There may be a slightly smaller effect of heading in the Bell, but its not significant (if the Hughes helicopter displayed heading differences in the 100's of nT there may have been a need to take corrective action).

Helicopter System Comparison

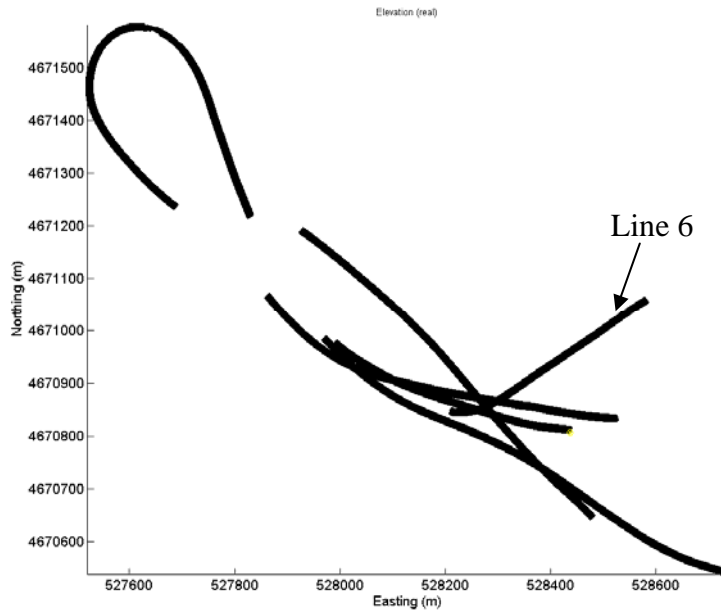


Figure 7: Plan view of the high altitude test-flight.

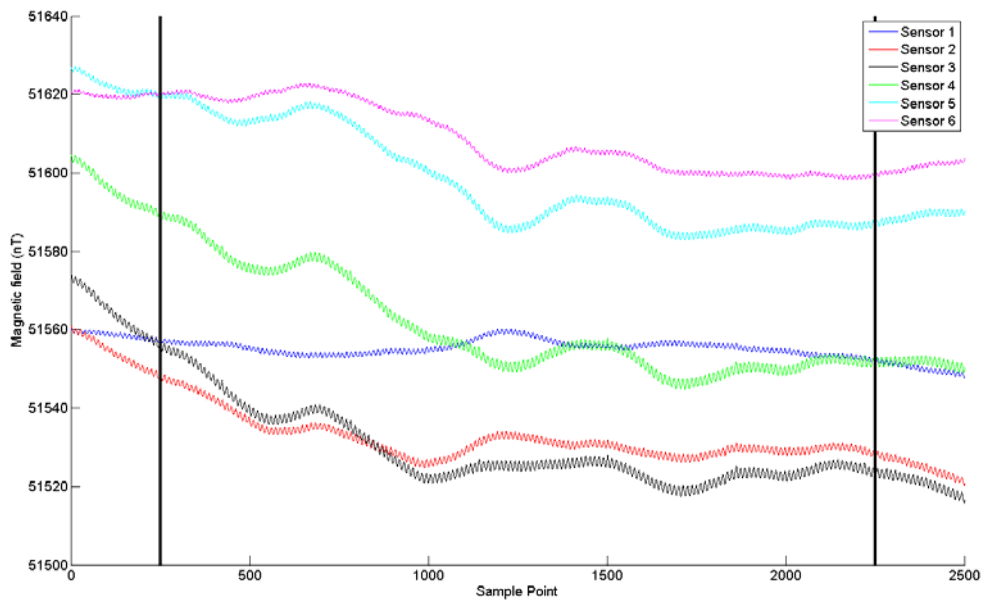


Figure 8: The 20 second data segment used for the characterization of the Hughes 530F with the Sky DAS.

Helicopter System Comparison

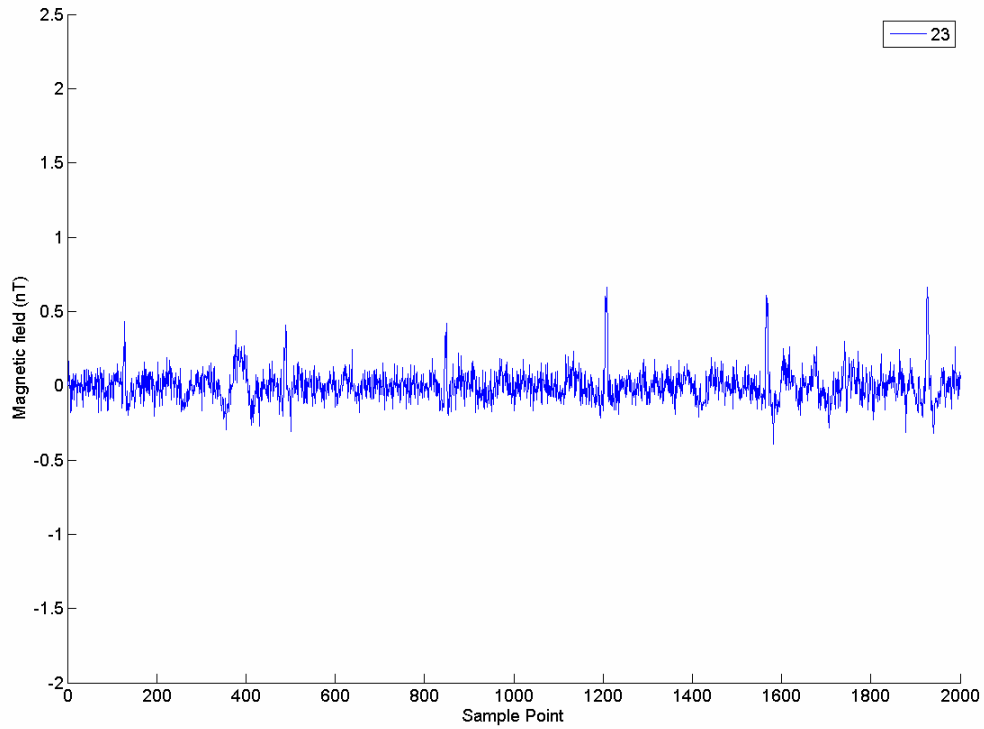
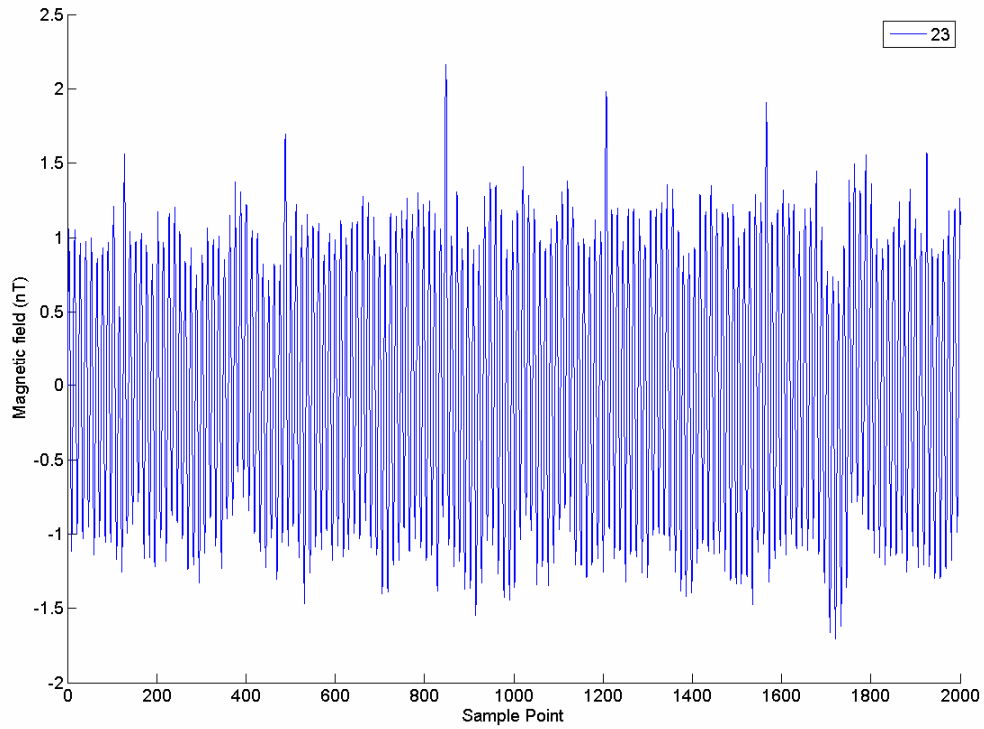


Figure 9: Detrend filtered data for sensor 4. Top row is minimally processed, bottom row is after applying a notch filter to suppress frequencies between 7 to 9 Hz.

Helicopter System Comparison

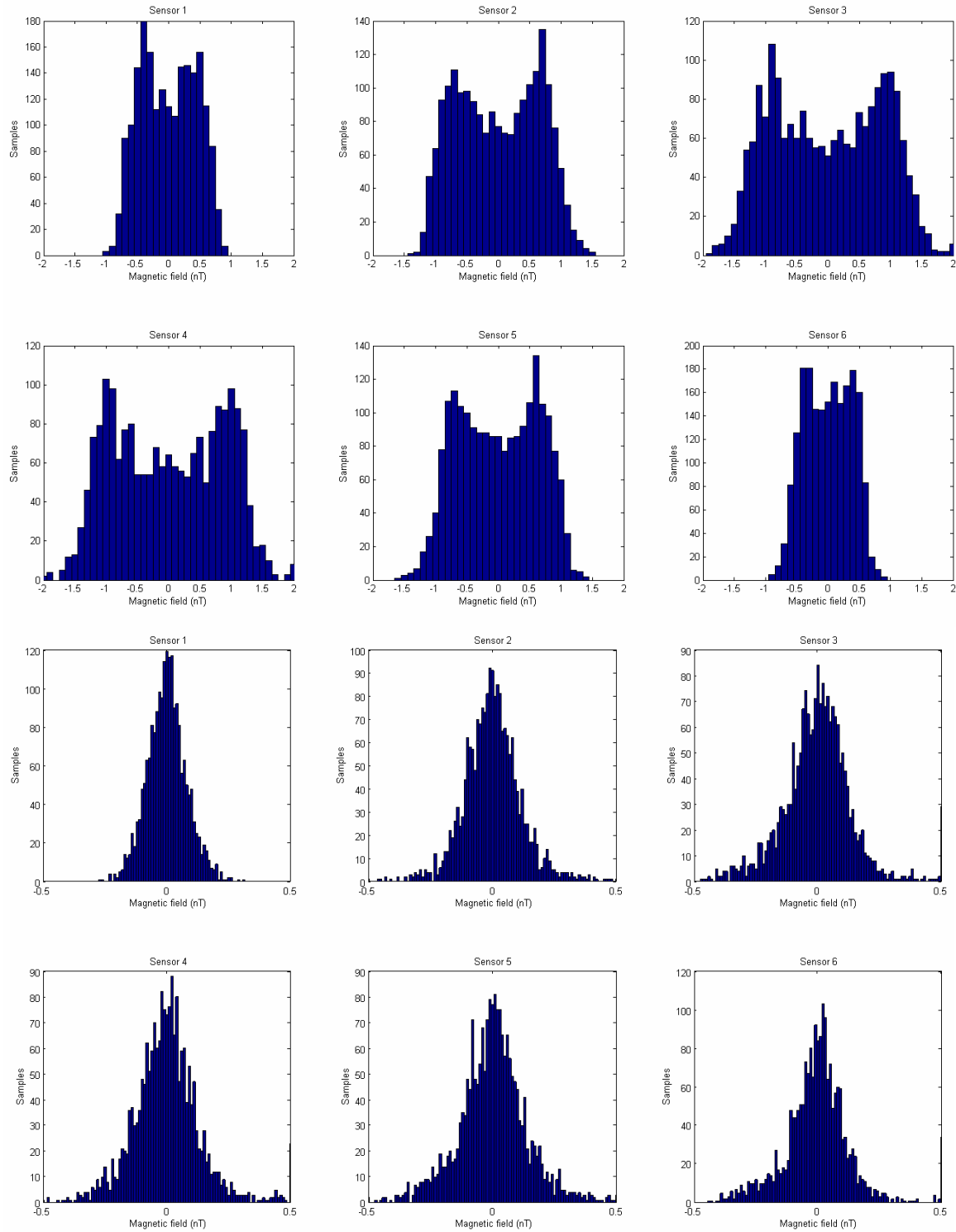


Figure 10: Histograms of detrend filtered data for the Sky DAS / Hughes combination. Top row is minimally processed, bottom row is after applying a notch filter to suppress frequencies between 7 to 9 Hz. See the Appendix for a description of why the minimally processed data is bimodal.

Helicopter System Comparison

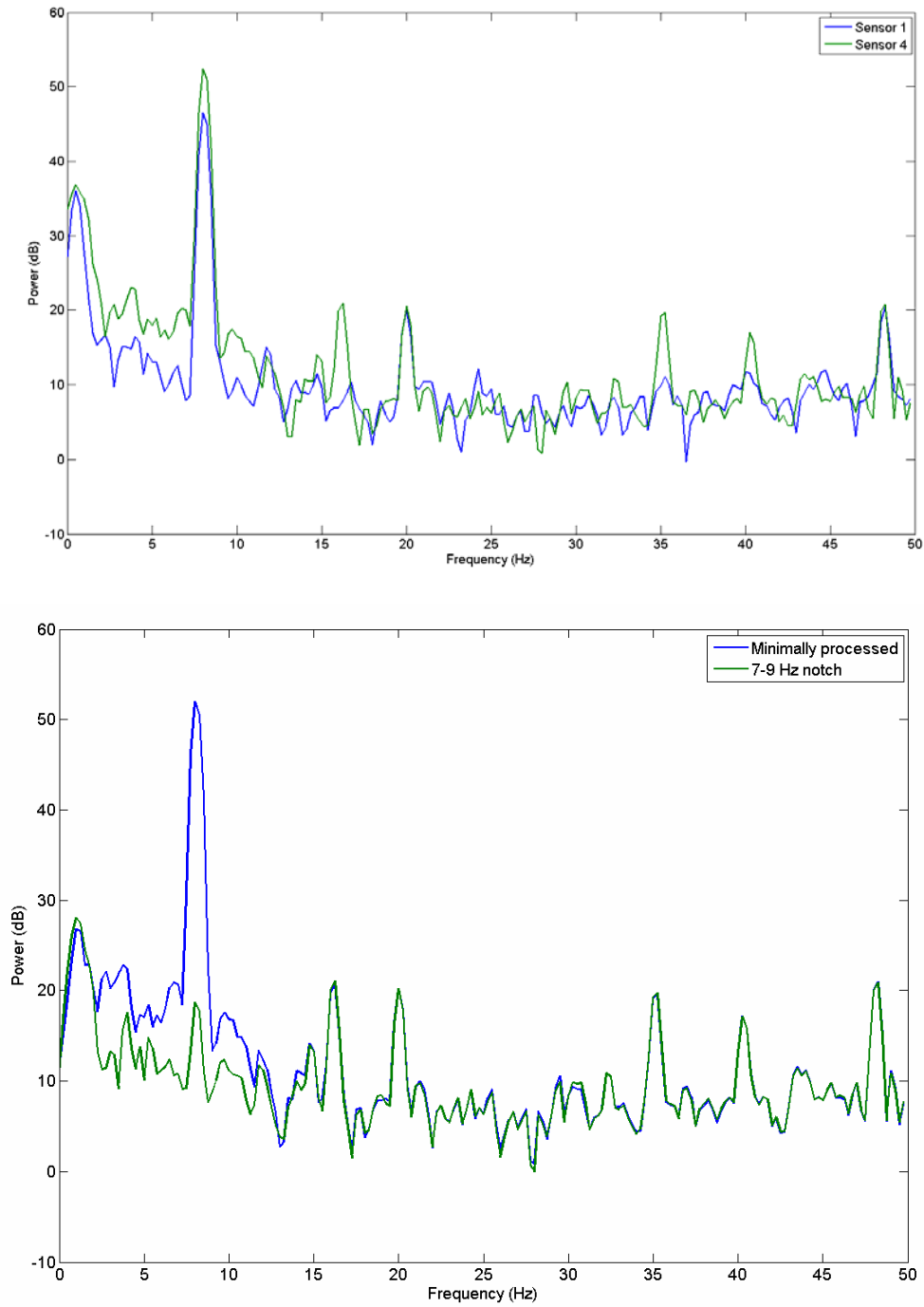


Figure 11: Top: Power spectrum of the minimally processed data from sensors 1 and 4. Bottom: Power spectrum of the minimally processed and notch filtered Sky HeliMag data.

Helicopter System Comparison

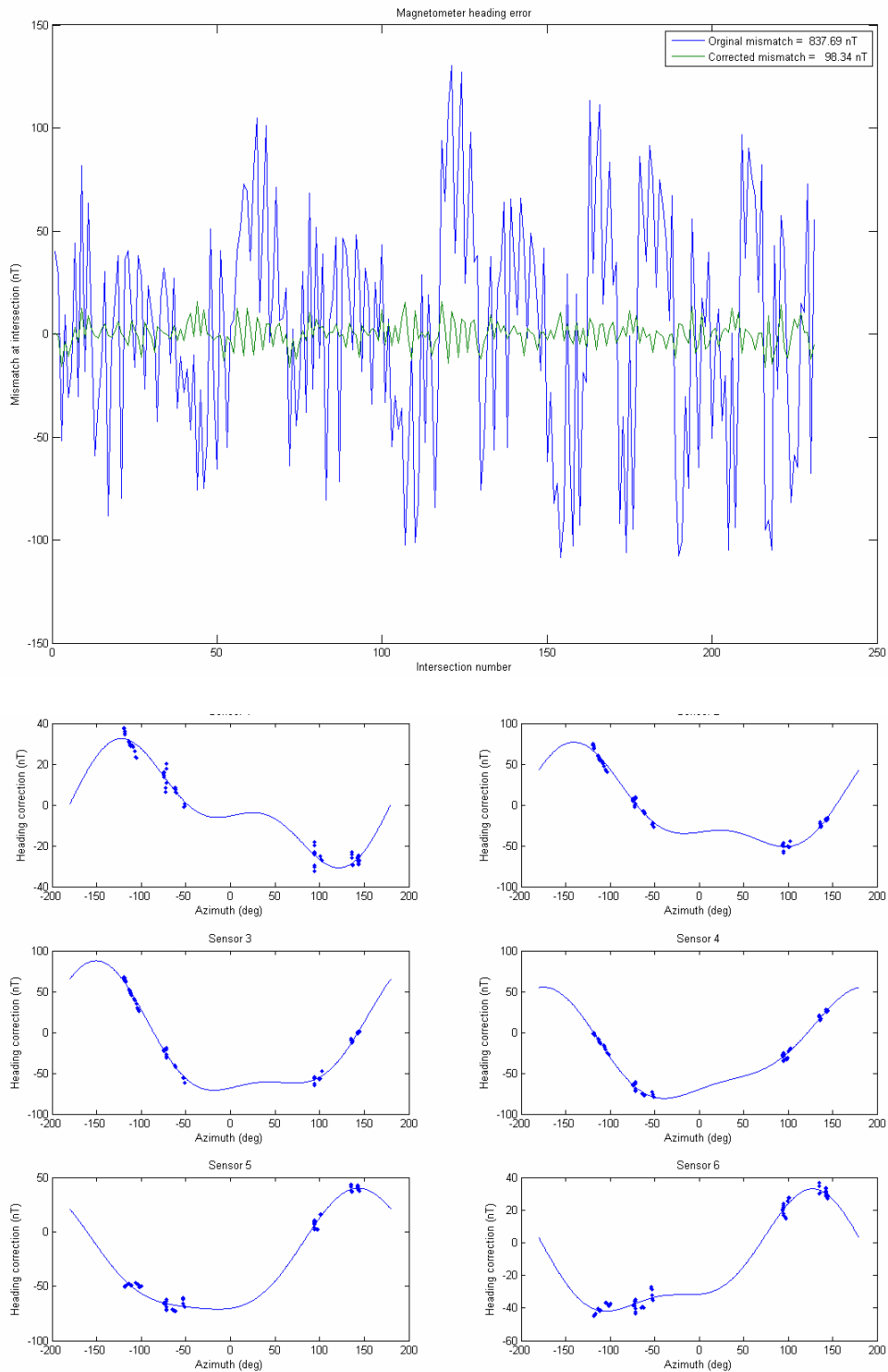


Figure 12: Analysis of the influence of the helicopter heading on magnetic field. At top we show the mismatch in recorded field values for each sensor at every intersection point. At bottom we show the heading correction for each sensor, along with the corrected mismatch at each sensor point.

Appendix A1: Why are the raw NRL and Sky histograms bimodal?

The power-spectrum analysis revealed that the dominant frequency of the noise was between 7 to 9 Hz. This relates to the rotation of the rotor in the helicopter. Now if we subtract the notch filtered data (from 7 to 9 Hz) from the minimally processed data, we get the histogram in Figure A1 below. This is bimodal with peaks at ± 1 nT, whereas the histogram of the notch filtered data was unimodal with zero mean (Figure 10 above). Thus we see that the 7-9 Hz noise from the rotor is the cause of the bimodal distribution. To see why this is the case, consider the histogram (Figure A2) of a uniformly sampled sinusoidal wave (the result for a sin or cosine is identical as they only differ by a 90 degree phase shift). The histogram is bimodal with modes at +1 and -1. This occurs because the maximum rate of change of the sinusoid occurs at zero amplitude, with the minimum rate of change at the positive and negative maxima. Thus, if there is a dominant sinusoidal noise source the histogram of the magnetic field will be bimodal. The peaks of the bimodal distribution will be at plus and minus values equal to the amplitude of the noise source.

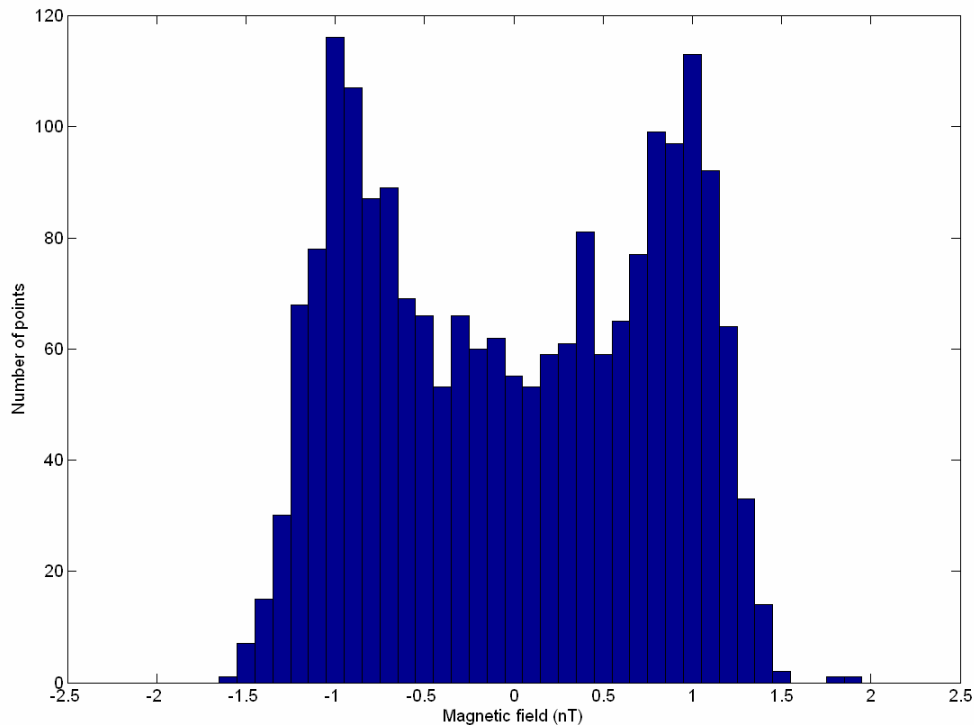


Figure A1: This histogram was obtained by subtracting the notch-filtered data from the minimally processed data for the Sky HeliMag system. Thus, it represents the effect of the 7-9 Hz noise.

Helicopter System Comparison

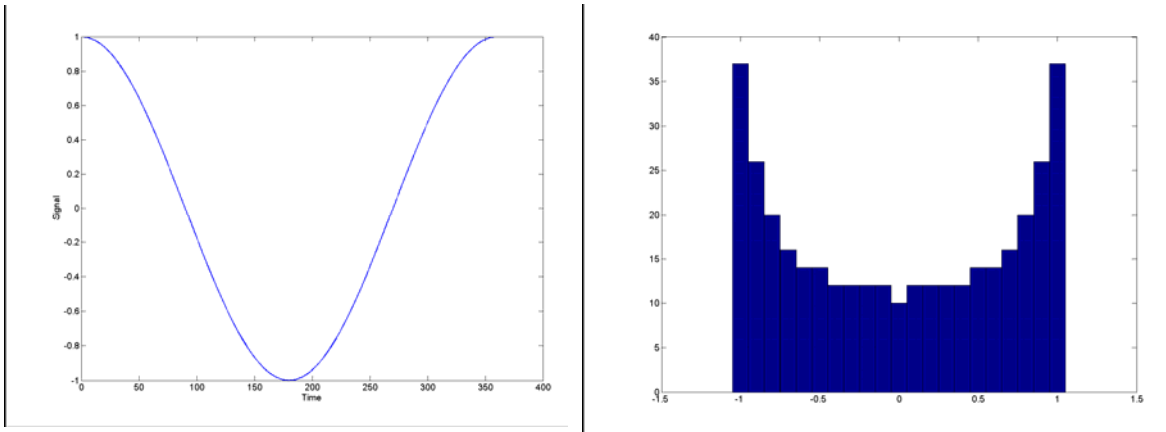


Figure A2: Graph of a sinusoidal signal and a histogram of the sinusoid when sampled uniformly (in this case at sample interval of $\pi/180$).

Appendix A2: More detailed analysis of Hughes 500 / Sky DAS system

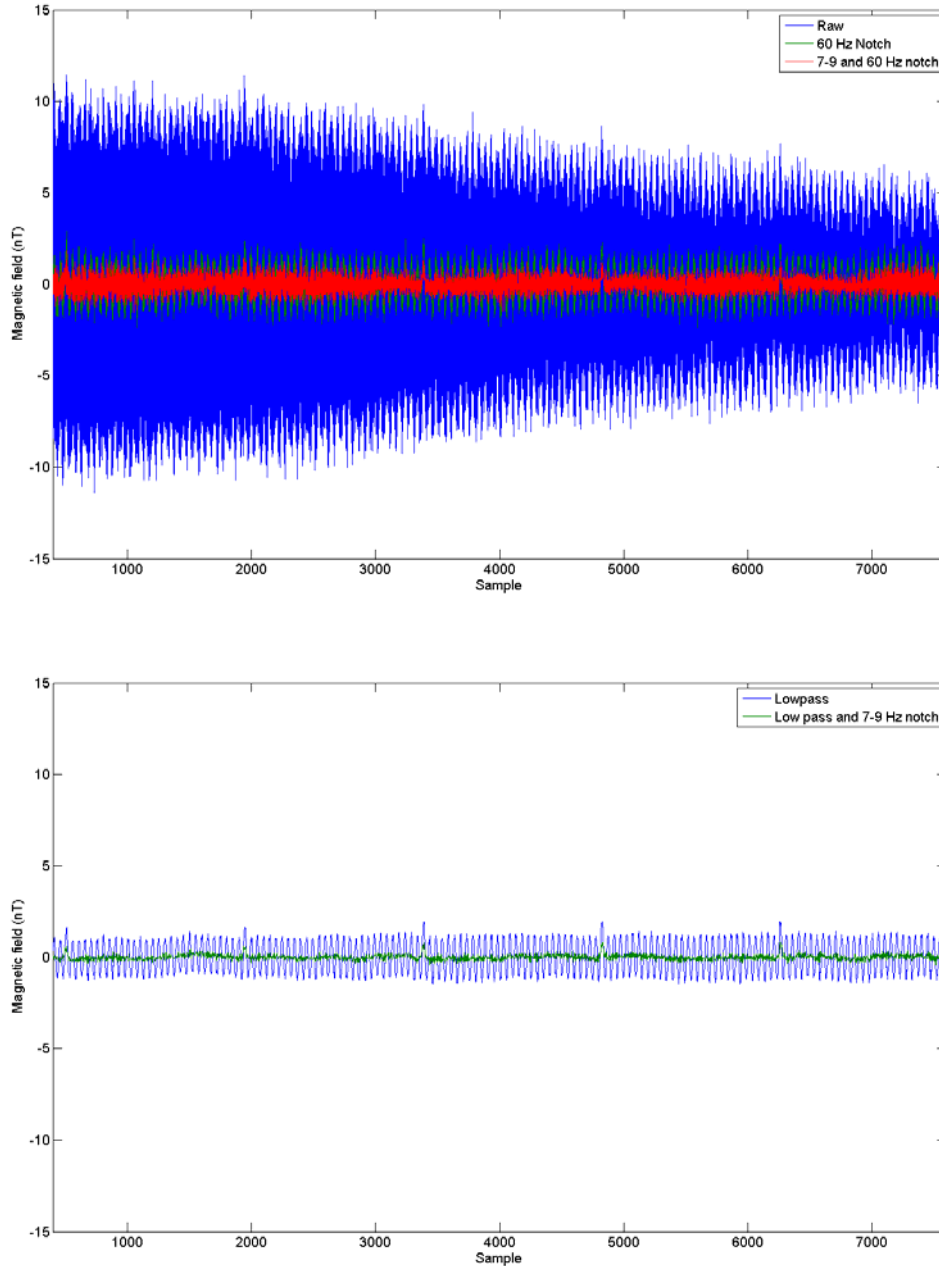


Figure B1: Profiles of the 20 second section of Sky data, at a sample rate of 400 Hz. Top row are for raw and two different notch filters. Bottom row is for low-pass filter with and without 7-9 Hz notch.

Helicopter System Comparison

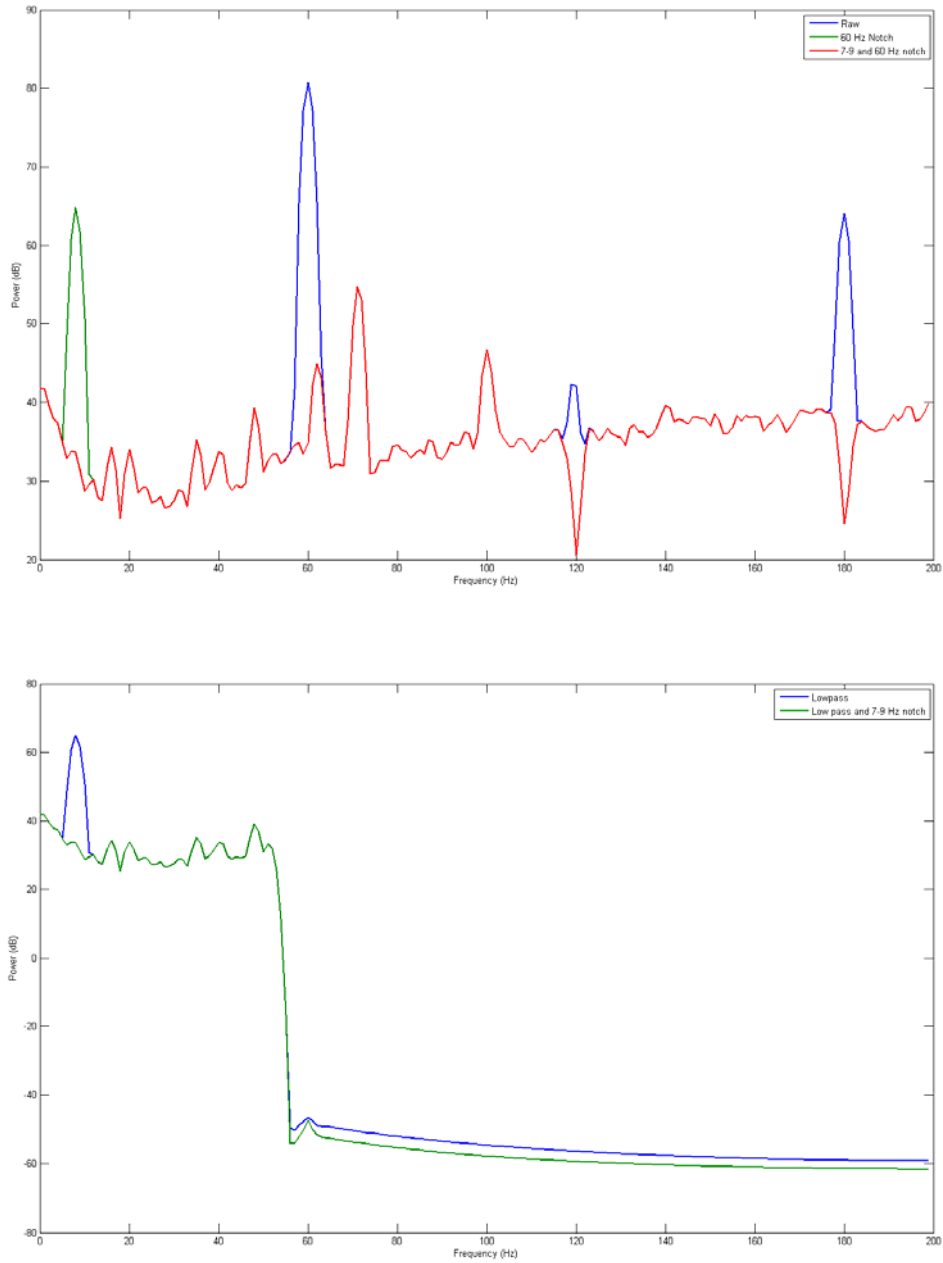


Figure B2: Power spectra of the 20 second section of Sky data, out to the Nyquist rate of 200 Hz. Top row are for raw and two different notch filters. Bottom row is for low-pass filter with and without 7-9 Hz notch.

Helicopter System Comparison

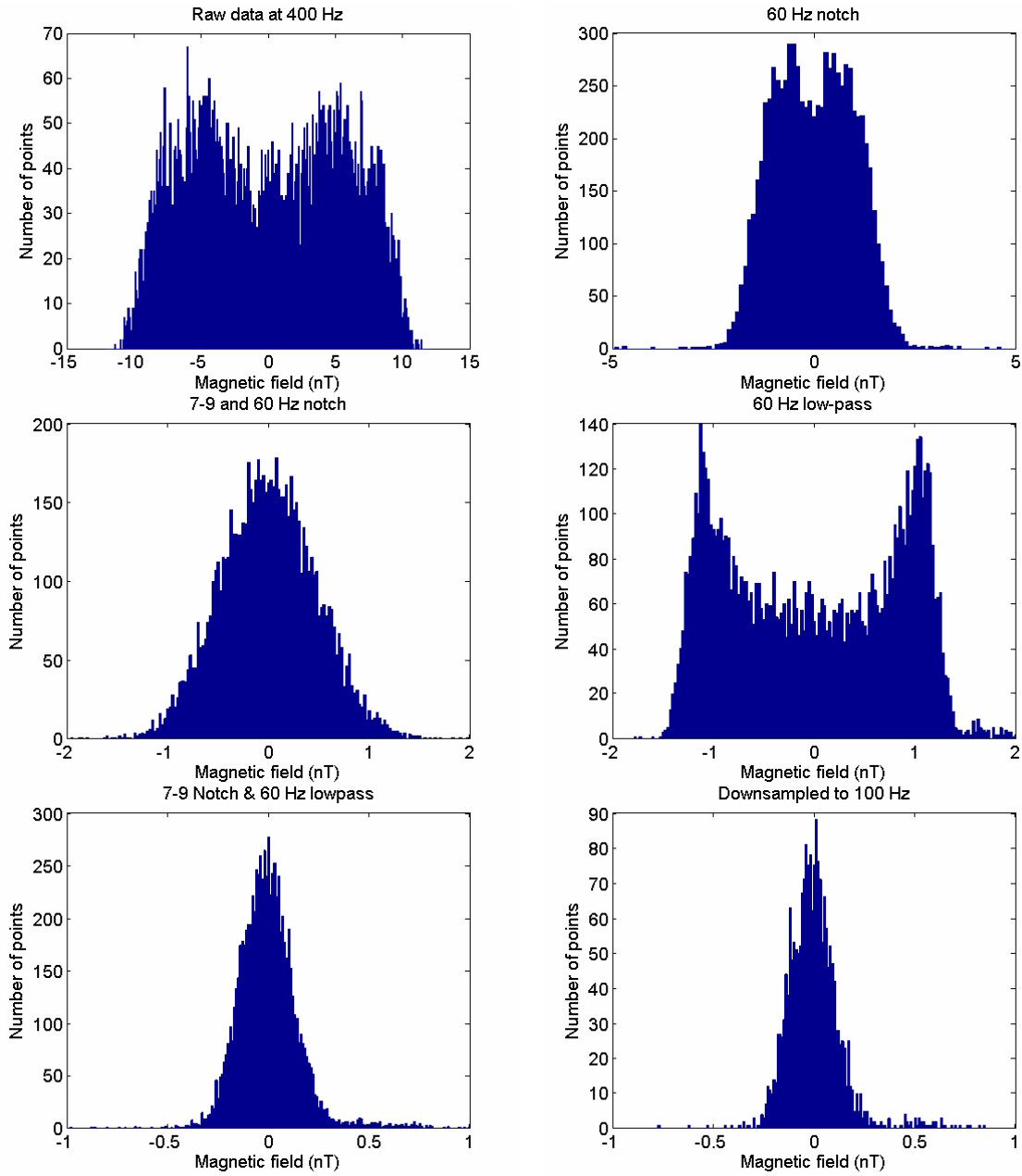


Figure B3: Histograms of the 20 second segment of Sky data for different levels of processing.

Table B1. Standard deviations of the data for different levels of processing. The last row is the closest to the NRL processing scheme.

Processing level	Std dev
Raw	5.52
Notch 60 Hz	0.96
Notch 7-9 & 60 Hz	0.46
Low pass 60 Hz	0.85
Notch 7-9 and Low-pass 60 Hz	0.14
Downsample to 100 Hz	0.12

APPENDIX B – RECOVERED TARGET RESULTS

GPS ID	OE_Type	Orientation	Attitude	Narrative	Sky ID	Fit Depth	Fit Moment	Fit Size	fit coherence
TRH-101	155 mm	Straight Down	Vert	155 mm below 2 Feet - Not recovered	101	2.63	3.69	0.191	0.900
TRH-103	155 mm	North	Hor	Mud Bottom	103	2.07	2.46	0.167	0.900
TRH-106	155 mm	N	Hor	Sand - Not Recovered – Fuzed	1	2.25	18.56	0.325	0.975
TRH-107	155 mm	N	Hor	Sand	2	1.88	17.15	0.317	0.983
TRH-109	155 mm	N	Hor	Sand / Mud	4	1.81	11.41	0.277	0.972
TRH-110	155 mm	Straight Down	Vert	Mud - Not Recovered	5	1.52	7.68	0.243	0.973
TRH-111	155 mm	N	Hor	Sand - Not Recovered – Fuzed	6	1.46	12.51	0.286	0.981
TRH-104	2.75 in Rocket	60 Deg Down	60 Deg Down	Hard Mud - Not Recovered - Assumed Fuzed	107	2.00	6.64	0.232	0.956
TRH-105	2.75 in Rocket	E	Hor	Mud - Not Recovered – Fuzed	115	2.51	3.08	0.180	0.935
TRH-100	NA	NA	NA	Contact below 2 feet	63	2.44	19.39	0.332	0.971
TRH-102	NA	NA	NA	Strong contact below 2 feet	102	1.28	1.65	0.147	0.855
TRH-114	NA	NA	NA	No Contact	10	1.13	16.47	0.315	0.988
TRH-115	NA	NA	NA	No Contact	11	1.13	7.14	0.238	0.981
TRH-117	NA	NA	NA	No Contact	14	0.92	20.33	0.335	0.993
TRH-108	Scrap	E	Hor	Sand - Metal Rod	3	1.58	10.56	0.270	0.983
TRH-112	scrap	W	Hor	Sand - 12 in dia pipe - too big to dig out	8	1.03	16.86	0.315	0.996
TRH-113	Scrap	E	Hor	Steel Can - Sand	9	1.01	13.30	0.292	0.992
TRH-116	Scrap	N	Hor	Steel I-beam - too big to dig out	13	0.65	8.17	0.248	0.986